Advances in Materials Science Research

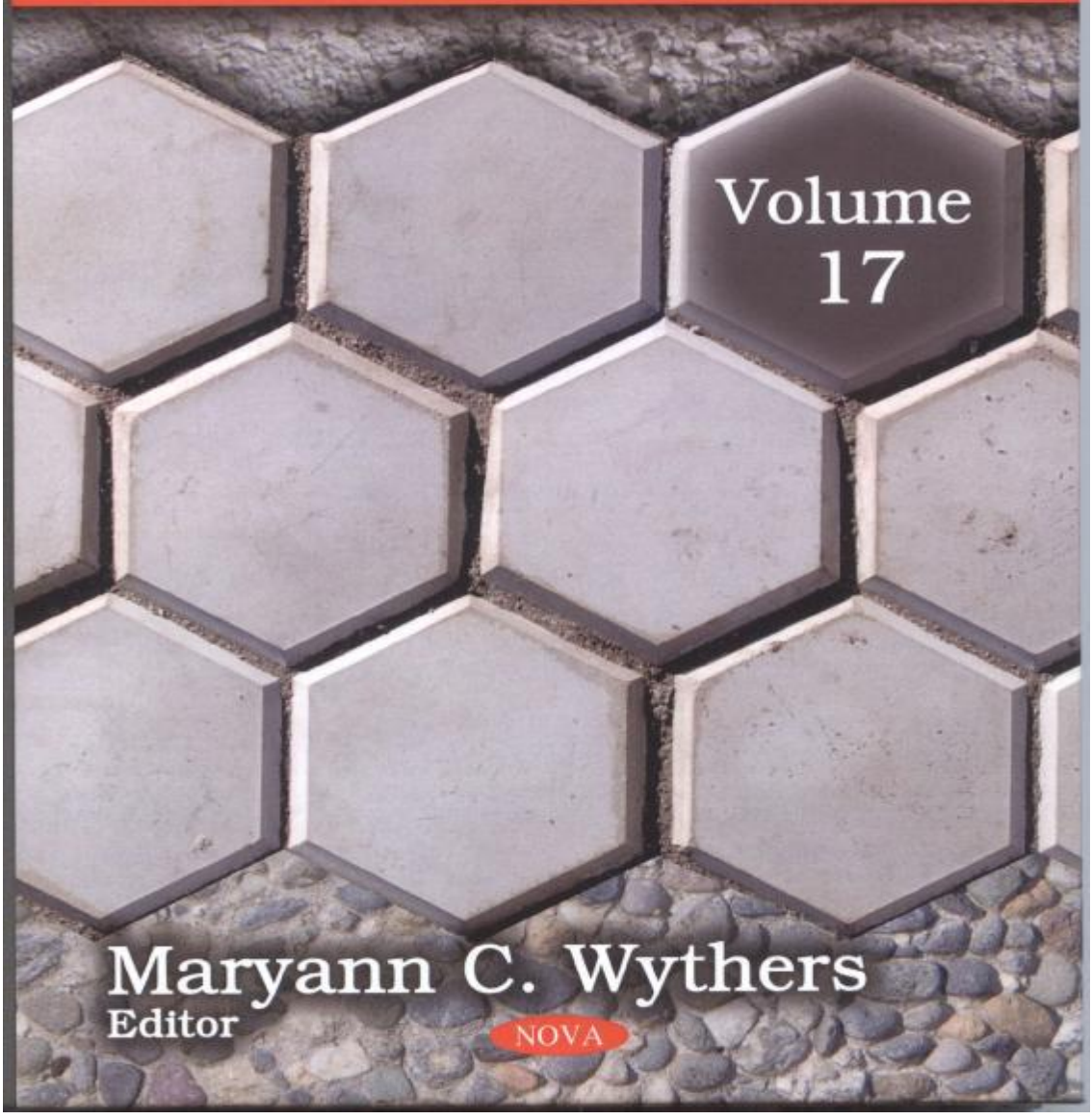

Maryann C. Wythers
Editor

NOVA

ADVANCES IN MATERIALS SCIENCE RESEARCH

Additional books in this series can be found on Nova's website under the Series tab.

\dditional e-books in this series can be found on Nova's websiti under the e-book tab.

ADVANCES IN MATERIALS SCIENCE RESEARCH

VOLUME 17

MARYANN C. WYTHERS Editor

nova publishers
New York

Library of Congress Cataloging-in-Publication Data

ISSN: 2159-1997 ISBN: 978-

1-62948-734-2

Published by Nova Science Publishers, Inc. f New York

CONTENTS

In: Advances in Materials Science Research… ISBN: 978-1-62948-734-2
Editor Maryann C. Wythers

Chapter 5

RELAXATION AND DYNAMICS OF SPIN CHARGE CARRIERS IN POLYANILINE

V.I. Krinichnyi*
Institute of Problems of Chemical Physics, Russian Academy of Sciences,
Moscow Region, Russian Federation

The main results of the study of charge transfer in polyaniline modified with sulfuric, hydrochloric, camphorsulfonic, 2-acrylamido-2-methyl-1-propanesulfonic and *para*-toluenesulfonic acids at various (9.7 – 140 GHz) wavebands EPR obtained in the Institute of Problems of Chemical Physics RAS are summarized. The methods of determining the composition of polarons with different mobility and their main magnetic, relaxation and dynamics parameters from effective EPR spectra are described. The dependences of the nature, electronic relaxation, dynamics of paramagnetic centers, and the charge transfer mechanism on the method of synthesis, the structure of the acid molecule, and the polyaniline oxidation level are shown.

Keywords: polyaniline, conducting polymers, EPR, spin, polaron, conducting mechanism, relaxation

* Institute of Problems of Chemical Physics, Russian Academy of Sciences, 142432 Chernogolovka, Moscow Region, Russian Federation. Fax: +7(496) 515 3588. E-mail: kivi@cat.icp.ac.ru

Within the class of conducting polymers, polyaniline (PANI), see Fig.1, is of special interest because of its excellent stability under ambient conditions and well perspective of utilization in molecular electronics [1,2]. The PANI family is known for its remarkable insulator-to-conductor transition as a function of protonation or oxidation level [3]. Depending on the protonation or oxidation level it can be in leucoemeraldine (LE), pernigraniline (PN), emeraldine base (EB), or emeraldine salt (ES) forms (Fig.1). PANI-LE is fully reduced state. PANI-PN is fully oxidized state with imine links instead of amine links. These two forms are poor conductors, even when doped with an acid. PANI-EB is neutral form, whereas PANI-ES is a *p*-type semiconductor with hole charge carriers [4]. It is semicrystalline, heterogeneous system with a crystalline (ordered) region embedded into an amorphous (disordered) matrix [5]. When PANI is doped with an acid, intermediate bipolaron and more stable polaron structures form as shown in Fig. 1. Such charge carriers transfer elemental charges during their intrachain and interchain diffusion as well as hopping inside and between well-ordered crystallites [6]. In polaron structure, a cation radical of one nitrogen acts as a hole and such holes acts as positive charge carriers. The electron from the adjacent nitrogen (neutral) jumps to this hole and it becomes electrically neutral initiating motion of the holes (Fig. 1). However, in bipolaron structure, this type of movement is not possible since two holes are adjacently located (Fig. 1). This polymer differs from polyacetylene (PA), poly(*para*-phenylene) (PPP), other PPP-like organic conjugated polymers in several important aspects. In contrast with these polymer systems it has no charge conjugation symmetry. Besides, both carbon rings and nitrogen atoms are involved in the conjugation. The phenyl rings of PANI can rotate or flip, significantly altering the nature of electron-phonon interaction. So, an additional mobility of macromolecular units can modulate sufficient electron-phonon interactions and, therefore, lead to more complex mechanism of electron transfer in PANI [7]. This results in somewhat of a difference in magnetic and charge-transport properties of PANI compared with other conducting polymers. Theoretically and experimentally was shown [8] that charges in PANI, as in case of other conducting polymers, are transferred by polarons moving along individual polymer chains. At low doping level a hopping charge transfer between polarons and bipolarons predominates in PANI. In modified polymer a number of such charge carriers increases and their energy levels merge and form metal-like band structure, so called polaron lattice [6,9]. Stronger spin-orbit and spin-lattice interactions of the polarons diffusing along the chains is also characteristic of PANI. Upon protonation of PANI-EB or oxidation of PANI-LE insulating forms of PANI their conductivity increases by more than 10 orders of magnitude whereas a number of electrons on the polymer chains remains constant

in the ES form of PANI [10]. Such a doping is accompanied by appearance of the Pauli susceptibility [11,12], characteristic for classic metals, due to formation of high-conductive completely protonated or oxidated clusters with the characteristic size about 5 nm in amorphous polymer. While doping of PANI-EB films with the sulfonated dendrimers gives direct current macroconductivity (σ_{dc}) up to ca. 10 S/cm, the hydrogensulfated fullerenol-doped materials show metallic characteristics with room temperature (RT) σ_{dc} as high as 100 S/cm [13] that is about 6 orders of magnitude higher than the typical value for fullerene-doped conducting polymers. In some cases diamagnetic bipolarons [6] and/or anti-ferromagnetic interacting polaron pairs [14] each possessing two elemental charges can also be formed in heavily doped polymer. The effective crystallinity of polymer increases up to ~ 50 – 60 %. The lattice constants of the PANI-EB and PANI-ES forms [5,9,15-17] are presented in Table 1.

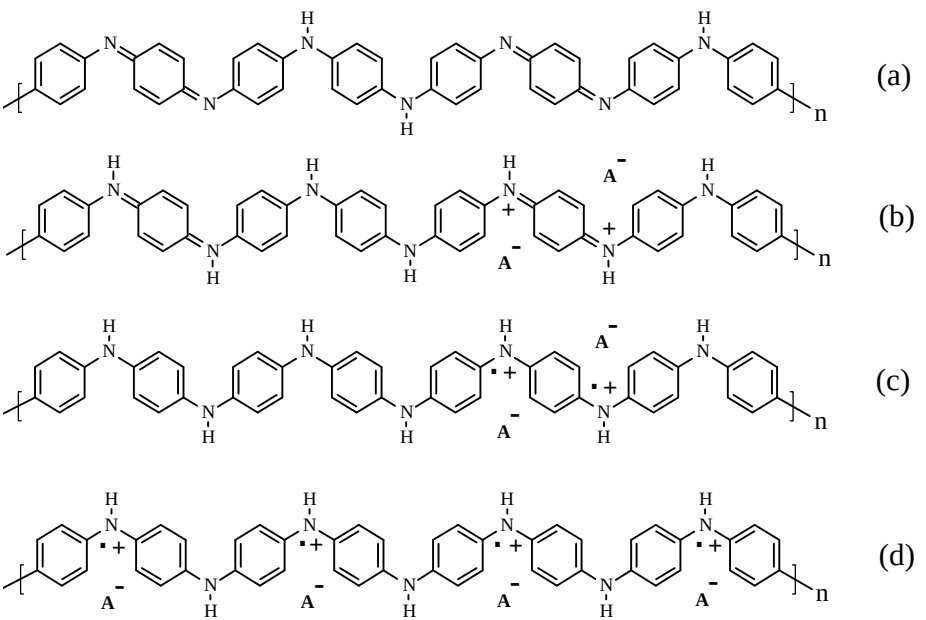

Figure 1. Chemical structures of emeraldine base (*a*) and its full (50%) protonation with formation of single bipolarons (*b*), polaron pairs (*c*) followed by their separation in more stable form (*d*).

Crystallinity and, therefore, conducting properties of PANI essentially depend on structure of a dopant introduced. The mechanism of charge transfer in heavily doped PANI is also dependent sufficiently on the nature of a dopant as well as on the method of the polymer synthesis. For instance, the Fermi level in PANI doped with sulphuric (PANI-SA) or hydrochloric (PANI-HCA) acid lies in the region of localized states, therefore is considered as a Fermi glass with localized electronic states [15], whereas the Fermi level energy ε_F of PANI highly doped with camphorsulphonic acid (PANI-CSA) lies in the region of extended states governing metal behavior of the latter near the metal-insulator boundary [18,19]. On the other hand, optical (0.06 – 6 eV) reflectance measurements of *e.g.* in PANI-CSA [15,20-22] suggest that this polymer is a disordered Drude-like metal near the metal-insulator boundary due to improved homogeneity and reduced degree of structural disorder. From optical measurements it was determined that the effective charge carrier mass $m^* \approx 2m_e$, the mean free path $l^* \approx 0.7$ nm and the density of states at the Fermi level $n(\varepsilon_F) \approx 1$ state per eV per two ring repeat units [15,20]. Studies of the effect of doping level on both the electronic transport and film morphology of PANI-CSA shown a direct correlation between the degree of crystallinity (induced by hydrogen bonding with the CSA counter ion) and the metallic electronic properties [23-25]. This leads to the improvement of crystallinity and metallic conductivity of the polymer in the series PANI-HCA $\rightarrow$ PANI-SA $\rightarrow$ PANI-CSA at comparable modification levels. However this deduction is not always conformed to results obtained at PANI study by other methods and other authors [26].

Table 1. Lattice constants (in nm) determined for polyaniline (PANI).

Polymer	*a*	*B*	*c*	Reference
PANI (e.b.)	0.765	0.575	1.020	[5]
PANI-HCA (e.s.)	0.705	0.860	0.950	[5]
PANI-SA (e.s., p.o.r.)	0.430	0.590	0.960	[9]
PANI-CSA	0.590	0.100	0.720	[15]
PANI-DBSA (o.r)	1.178	1.791	0.716	[16]
PANI-*p*TSA	0.440	0.600	1.100	[17]

Abbreviations: e.b. – emeraldine base, e.s. – emeraldine salt, p.o.r. - pseudo-orthogonal cell, o.r. – orthrombic cell, HCA - hydrochloric acid, SA - sulphuric acid, CSA - camphorsulphonic acid, DBSA - dodecylbenzenesulphonic acid, *p*TSA - *p*-toluenesulfonic acid.

Typical *dc* conductivity is frequently a result of various electronic transport processes and is ca. 10 – 10^2 S/cm for disoriented and oriented PANI-ES [3,10,18,27-34]. For example, this value has been determined for PANI-CSA to be in the range $\sigma_{dc} \approx 1.0 \cdot 10^2 - 3.5 \cdot 10^2$ S/cm at room temperature [33,35]. The variety of conducting properties makes difficult to investigate completely and correctly by usual experimental methods true charge dynamics along a polymer chain, which can be masked by interchain, interglobular and other charge transfer processes. The inhomogeneity of distribution of the counterion molecules results in an additional complexity of experimental data interpretation.

The electronic structure of PANI-ES has been described theoretically by the metallic polaron lattice model [6,36] with a finite $n(\varepsilon_F)$ value [37]. An analysis of experimental data on the temperature dependencies of *dc* conductivity, thermoelectric power, and Pauli-like susceptibility allowed MacDiarmid, Epstein *et al.* [27,30,38-41] to declare that PANI-EB is completely amorphous insulator in which 3D granular metal-like domains of characteristic size of 5 nm are formed during its doping and transformation into PANI-ES. A more detailed study of the complex MW dielectric constant, EPR line width, and electric field dependence of conductivity of PANI-ES [5,9,27,28,30,42] allowed them to conclude that both chaotic and oriented PANI-ES consist of some parallel chains strongly coupled into "metallic bundles" between which ID VRH charge transfer occurs and in which 3D electron delocalization takes place. The intrinsic 3D conductivity of the domains was evaluated using Drude model [43] at alternating current as $\sigma_{ac} \cong 10^7$ S/cm at 6.5 GHz [44], which was very close to the value expected by Kivelson and Heeger for the metal-like clusters in highly doped Naarmann *trans*-PA [45]. However, *ac* conductivity of the sample does not exceeds $\sigma_{ac} \cong 7 \cdot 10^2$ S/cm [44]. It means that other processes, which make difficult its determination, mask the true process of electron transfer by usual experimental methods.

The polaronic charge carriers in PANI and other conducting polymers are characterizing by electron spin S = ½, so then the Electron Paramagnetic Resonance (EPR) method is widely used for the study of relaxation and dynamics properties of such paramagnetic centers (PC) in these systems [46-49]. The oxidation or protonation of PANI-EB leads to the monotonically increase in PC concentration accompanied with the 3-cm waveband EPR line narrowing from 2 G down to 0.5 G [50,51]. Lapkowski *et al.* [51] and MacDiarmid and Epstein [52] showed the initial creation of Curie spins in EB, indicating a polaron formation, followed by a conversion into Pauli spins, which shows the formation of the polaron lattice in high conductive PANI-ES [53,54]. The method enables to determine both the spin-lattice and spin-spin relaxation occurring with the times

T_1 and T_2, respectively, as well as the diffusion of spin charge carriers along and between chains with appropriate coefficients D_{1D} and D_{3D}, respectively, even in PANI with chaotically oriented chains in scale from several macromolecular unites [46,47]. These parameters are important to understand how relaxation and transport properties of spin charge carriers depend on the structure and dynamics of their microenvironment (lattice, anion *etc.*). It should be noted that diffusion of electron spin effects nuclear relaxation of protons in PANI, so in principle the Nuclear Magnetic Resonance (NMR) spectroscopy can additionally be used for the study of electron spin dynamics in PANI [55]. Such investigations were mainly carried out for highly doped PANI-HCA [56-60]. It was noted, however, [47], that the data on PANI proton relaxation experimentally obtained by NMR method [56-58], reflect an electron spin dynamics indirectly and consequently cannot give a correct enough conception of charge transfer in polymer. On the other hand, EPR method registers just electron relaxation of spin charge carriers, that allows more precisely to determine relaxation and dynamic parameters of polarons in PANI and in others conducting polymers.

Spin-spin relaxation of polarons governs their peak-to-peak EPR line width ΔB_{pp} at electron spin precession frequency ω_e. The dependencies $T_1 \propto \omega_p^{1/2}$ (here ω_p is the angular frequency of nuclear spin precession) and $\Delta B_{pp} \propto \omega_e^{1/2}$ obtained respectively for nuclear and electron spins by comparatively low-frequency EPR and NMR methods for highly protonated PANI-ES were interpreted in terms of 1D diffusion and 3D hopping of a polaron. D_{1D} value was obtained to be respectively near to 10^{14} and 10^{12} rad/s and weekly depend on the doping level, while D_{3D} value strongly depends on y and correlated with both *dc* and *ac* conductivities of PANI-HCA [56]. The anisotropy of this motion $A = D_{1D}/D_{3D}$ varies at room temperature from 10^4 in PANI-EB down to 10 in PANI-ES. This fact was interpreted in favor of existence even in highly protonated PANI of single high-conductive chains, between which Q1D charge transfer is realized [61]. Such an interpretation differs from the alternate model of formation of Q3D metal-like clusters in amorphous phase of the polymer [38,39]. Besides, the diffusion constants were determined from EPR line width which may reflect different processes carrying out in PANI. Indeed, at registration frequencies less than 10 GHz the lines of multicomponent spectra or spectra of different radicals with close magnetic resonance parameters overlap due mainly to low spectral resolution. So, line width of PANI at these frequencies generally represents a superposition of various contributions of localized and delocalized PC.

The presence in the PANI of oxygen molecules can also affect its magnetic resonance parameters. In this case the change in line width of organic systems is

normally explained by dipole-dipole interaction of polarons with spin $S = ½$ with the oxygen molecules possessing sum spin $S = 1$. It was found [62-66] that oxygen can reversibly broad EPR spectrum of PANI without remarkable change of its conductivity. Previous vacuumization of the sample leads to more promising effect that is characterized by relaxation time of spin-spin interaction [66-69]. However, Kang et al. have shown [70] that the contact of PANI-HCA with air leads to reversible decrease in the intensity and increase in the width of the EPR spectrum of PANI at simultaneous decrease in its conductivity. Such change in the polymer properties was explained by the decrease of the polaron mobility at its interaction with air. The opposite effect, however, was registered in the study of polypyrrole [71] and PANI-HCA [72]. In the latter case the diffusion of the oxygen into the polymer was proposed to lead to reversible increase in the polymer line width and conductivity due to acceleration of a polaron motion along the polymer chain.

As in case of other conducting polymers, some highly doped PANI samples demonstrate EPR spectra with Dyson contribution [73] as result of interaction of MW field with spin or/and spineless charge carriers [74,75]. This additionally results in ambiguous interpretation of the data obtained on electron relaxation and dynamics, and also on mechanism of charge transport in conducting polymers.

In the present Chapter are considered the results of multifrequency EPR study of magnetic and charge transport properties of PANI-EB and PANI-ES doped with different acids up to $y \leq 0.60$ [48,76-91]. Powder-like PANI-SA was synthesized by polymerization via a modification of the general oxidation route with $(NH_4)_2S_2O_8$ in 1.0 M hyrochloric acid which was doped into aqueous solution of sulfuric acid with an appropriate *p*H value [92]. PANI-HCA was synthesized by the chemical oxidative polymerization of 1 M aqueous solution of polyaniline sulfate in the presence of 1.2 M ammonium persulfate at 278 K [93]. Film-like high-molecular-weight polyaniline synthesized in Durham at 248 K [94,95] was used as an initial material for PANI-ES doped with CSA and 2-acrylamido-2-methyl-1-propanesulphonic (AMPSA) as films of ~50 μm thick which were cast from *m*-cresol or dichloroacetic acid solutions onto Si wafers and allowed to dry in air at 313 K [94,96]. It was studied also powder-like *para*-toluenesulfonic-acid-doped PANI-ES (PANI-*p*TSA) with $y = 0.5$ doping level and 30% crystalline volume fraction [17].

Figure 2 shows 3-cm ($\nu_e = \omega_e/2\pi = 9.7$ GHz) and 2-mm ($\nu_e = 140$ GHz) waveband EPR spectra of an initial, PANI-EB sample, and PANI slightly doped with different numbers of sulfuric acid molecules. At the 3-cm waveband PANI-EB demonstrates a Lorentzian three-component EPR signal consisting of asymmetric (R_1) and symmetric (R_2) spectra of paramagnetic centers which should be attributed

respectively to localized and delocalized PC (Fig.2,a). R_2 PC keep line symmetry at higher doping levels. At the 2-mm waveband the PANI EPR spectra became Gaussian and broader compared with 3-cm waveband ones (Fig.2,b), as is typical of PC in other conducting polymers [49,79]. At this waveband delocalized PC demonstrate an asymmetric EPR spectrum at all doping levels. The analysis of EPR spectra obtained at both wavebands EPR showed that the line asymmetry of R_2 PC in undoped and slightly doped PANI samples can be attributed to anisotropy of the *g*-factor which becomes more evident at the 140 GHz waveband EPR. The line width of these PC weakly depends on the temperature.

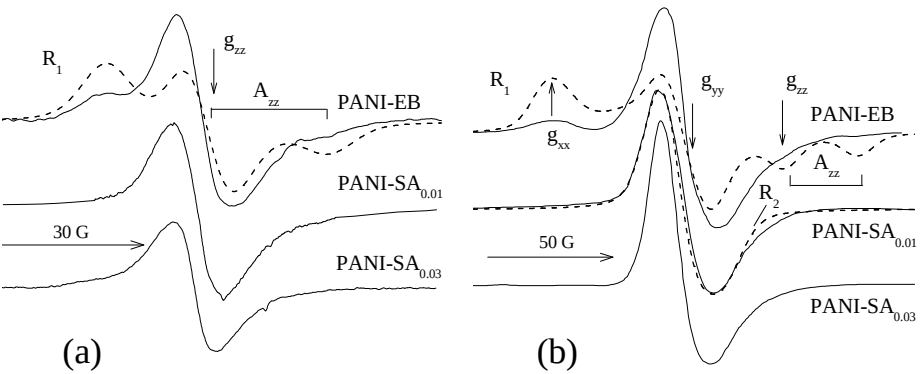

Figure 2. Typical room temperature 3-cm (*a*) and 2-mm (*b*) waveband EPR absorption spectra of PANI-EB and this sample slightly doped by sulphuric acid. The absorption spectra calculated with $g_{xx}= 2.0060_{32}$, g_{yy} 2.0038_{15}, $g_{zz} = 2.0023_{90}$, $A_{xx} = A_{yy} = 4.5$ Gauss, $A_{zz} = 0.2$ Gauss (R_1), and with $g_{\perp} = 2.0043_{94}$ and $g_{\parallel} = 2.0037_{63}$ (R_2) are shown by dashed lines.

Therefore, the R_1 with strongly asymmetric EPR spectrum can be attributed to a — (Ph-$\overset{\bullet}{\underset{}{\text{NH}}}^{+}$-Ph)— radical with $g_{xx} = 2.0060_{32}$, $g_{yy} = 2.0038_{15}$, $g_{zz} = 2.0023_{90}$, $A_{xx}=A_{yy} = 4.5$ G, and $A_{zz} = 30.2$ G, localized on a short polymer chain. The magnetic parameters of this radical differ weakly from those of the Ph-$\overset{\bullet}{\text{NH}}$-Ph radical [97], probably because of a smaller delocalization of an unpaired electron on the nitrogen atom ($\rho_N^{\pi} = 0.39$) and of the more planar conformation of the latter. Assuming a McConnell proportionality constant for the hyperfine interaction of the spin with nitrogen nucleus $Q = 23.7$ G [97], a spin density on the heteroatom nucleus of $\rho_N(0) = (A_{xx}+A_{yy}+A_{zz})/(3Q) = 0.55$ is estimated. At the same time another radical R_2 is formed in the system with $g_{\perp} = 2.0043_{94}$ and $g_{\parallel} = 2.0037_{63}$

which can be attributed to PC R_1 delocalized on more polymer units of a longer chain. Indeed, the model spectra presented in Fig.2 well fit both the PC with different mobility. The lowest excited states of the localized PC were determined from equation [97,98]

$$\begin{vmatrix} g_{xx} & & \\ & g_{yy} & \\ & & g_{zz} \end{vmatrix} = \begin{vmatrix} 2\left(1+\frac{\lambda\rho(0)}{\Delta E_{n\pi^*}}\right) & & \\ & 2\left(1+\frac{\lambda\rho(0)}{\Delta E_{\sigma\pi^*}}\right) & \\ & & 2 \end{vmatrix} \quad (1)$$

where λ is the spin-orbit coupling constant, $\rho(0)$ is the spin density, $\Delta E_{n\pi^*}$ and $\Delta E_{\sigma\pi^*}$ are the energies of the unpaired electron $n\rightarrow\pi^*$ and $\sigma\rightarrow\pi^*$ transitions, respectively, to be $\Delta E_{n\pi^*}$ = 2.9 eV and $\Delta E_{\sigma\pi^*}$ = 7.1 eV at ρ^{π}_{N} = 0.56 [99]. In PANI-HCA the R_1 also demonstrates the strongly anisotropic spectrum with the canonic components $g_{xx}= 2.0052_2$, $g_{yy}= 2.0040_1$, and $g_{zz}= 2.0022_8$ of $\boldsymbol{g}$ tensor, and hyperfine coupling constant A_{zz} = 22.7 G. Radicals R_2 are registered at $g_{\perp} =2.0046_3$ and $g_{\parallel} = 2.0022_3$.

It was shown earlier [100,101] that g_{xx} and A_{zz} values of nitroxide radicals localized in a polymer are sensitive to changes in the radical microenvironmental properties, for example polarity and dynamics. The shift of the PC R_2 spectral X component to higher fields with y and/or a temperature increase may be interpreted not only by the growth of the polarity of the radical microenvironment, but also by the acceleration of the radical dynamics near its main molecular X axis. The effective g-factors of both PC are near to one another, i.e. $\langle g_1\rangle = 1/3(g_{xx} + g_{yy} + g_{zz}) \approx \langle g_2\rangle = 1/3(g_{\parallel}+2g_{\perp})$. This indicates that the mobility of a fraction of radicals R_1 along the polymer chain increases with the polymer doping. Such a depinning of the mobility results in an exchange between the spectral components of the PC and, hence, to a decrease in the anisotropy of its EPR spectrum. In other words, radical R_1 transforms into radical R_2, which can be considered as a polaron diffusing along a polymer chain with a minimum diffusion rate [102]

$$D^0_{1D} \geq \frac{(g_{\perp} - g_e)\mu_B B_0}{\mathbf{h}}, \quad (2)$$

giving D_{1D}^{0} = 6.5·10^{8} rad/s.

As in case of other conducting polymers, at the 2-mm waveband in both in-phase and π/2-out-of-phase components of the dispersion EPR signal of neutral and slightly doped PANI, the bell-like contribution with Gaussian spin packet distributions due to the adiabatically fast passage of the saturated spin packets by a modulating magnetic field is registered (insert of Fig.3,b). This effect was not observed earlier in studies of PANI at lower registration frequencies [103]. It can be used for determining of relaxation and dynamics parameters of these PC.

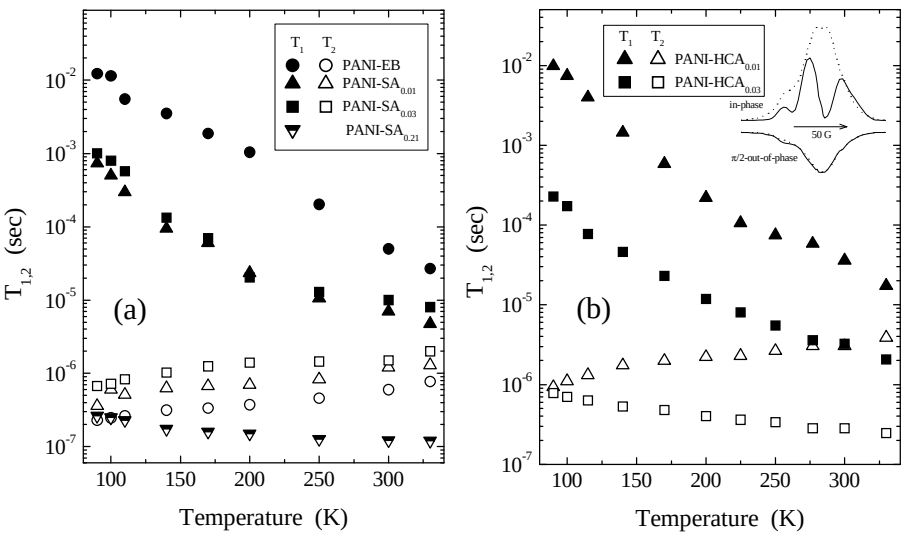

Figure 3. Temperature dependences of the effective spin-lattice and spin-spin relaxation times of polarons in undoped, PANI-EB, (*a*) as well as in PANI-SA and PANI-HCA (*a*,*b*) samples with different doping levels. In the insert (*b*) are shown typical 2-mm waveband EPR in-phase and π/2-out-of-phase dispersion spectra of PANI-EB registered at room temperature (solid line) and 200 K (dotted line).

The relaxation times of adiabatically saturated PC in π-conducting polymers can be determined separately from the analysis of the u_1-u_3 components of its dispersion spectrum as [104,105]

$$T_1 = \frac{3\omega_m(1+6\Omega)}{\gamma_e^2 B_{1_0}^2 \Omega(1+\Omega)}, \qquad (3)$$

$$T_2 = \frac{\Omega}{\omega_m} \tag{4}$$

(here ω_m is the *ac* modulation frequency, $\Omega = u_3/u_2$, B_{1_0} is the MW polarizing field at which the condition $u_1 = -u_2$ is valid) at $\omega_m T_1 > 1$ and

$$T_1 = \frac{\pi u_3}{2\omega_m u_1}, \tag{5}$$

$$T_2 = \frac{\pi u_3}{2\omega_m (u_1 + 11u_2)} \tag{6}$$

at $\omega_m T_1 < 1$. The amplitudes of u_i components are measured in the central point of the spectra, when $\omega = \omega_e$.

Relaxation times of an initial, PANI-EB, and slightly doped PANI-SA and PANI-HCA samples calculated from Eqs.(3) to (6) are shown in Fig.3 as functions of temperature. The Figure demonstrates that the increase in the doping level of the polymer leads to shortening of the effective relaxation times of PC, which can be due to an intensification of the spin exchange with the lattice and with other spins stabilized on neighboring polymer chains of highly conducting domains. It should be noted that spin relaxation in the polymer at high temperatures are mainly determined by the Raman interaction of the charge carries with lattice optical phonons. The probability and rate of such a process are dependent on the concentration n of the PC localized, e.g., in ionic crystals ($W_R \propto T_1^{-1} \propto n^2 T^7$) and in π-conjugated polymers ($W_R \propto T_1^{-1} \propto nT^2$) [106]. The available data suggest that the T_1^{-1} values of PC in slightly (up to $y \leq 0.03$) doped PANI are described by a dependence of the type $T_1^{-1} \propto nT^k$, where $k = 3 - 4$. The k exponent decreases with the y increase. This indicates the appearance of an additional channel of the energy transfer from the spin ensemble to the lattice at the polymer doping, as is the case in classical metals. At a medium degree of oxidation $y \geq 0.21$, the electronic relaxation times become comparable and only slightly temperature dependent because of an intense spin-spin exchange in metal-like domains of higher effective dimensionalities. Providing that $T_1 = T_2$ for the PANI sample with $y = 0.21$, an effective rate of Q1D and Q2D spin motions in this

polymer can be evaluated as well. It seems that both the rates calculated in the frameworks of such spin diffusions should be near to one another.

The shape of π/2-out-of-phase dispersion signal of PC localized in PANI-EB changes with the temperature (insert of Fig.3,b) indicating the defrosting of anisotropic macromolecular librations in this polymer. The correlation of such motions was determined as [46,49]

$$\tau_c^{x,y} = \tau_{c0}^{x,y} \left(u_3^{x,y} / u_3^{y,x} \right)^{-\alpha}, \tag{7}$$

(here α is a constant determining by an anisotropy of *g*-factor) with τ_{c0}^{x} = 5.4·10^{-8} sec and α = 4.8 to be τ_c^{x} =3.5·10^{-5}exp(0.015 eV/$k_B T$). Similar dependencies were also obtained for slightly doped samples. The activation energy of the polymer chains librations lies near to that determined for PANI-HCA [80]. Upper limit for correlation time was determined R_1 to be equal to 1.3·10^{-4} sec and corresponds to u_3^{x} / u_3^{y} = 0.22 in Eq.(7) at 125 K.

The relaxation times of electron and proton spins in PANI should vary depending on the spin precession frequency as $T_{1,2} \propto n^{-1} \omega_e^{1/2}$ [56]. This is a case for PANI-SA and PANI-HCA, therefore, the experimental data obtained for these polymers can be explained by a modulation of electronic relaxation by Q1D diffusion of R_2 radicals along the polymer chain, and by Q3D hopping of these centers between chains with the diffusion coefficients D_{1D} and D_{3D}, respectively.

Both the diffusion coefficients D_{1D} and D_{3D} can be calculated from relations [98,107]

$$T_1^{-1} = \langle \Delta\omega^2 \rangle \left[2J(\omega_e) + 8J(2\omega_e) \right], \tag{8}$$

$$T_2^{-1} = \langle \Delta\omega^2 \rangle \left[3J(0) + 5J(\omega_e) + 2J(2\omega_e) \right], \tag{9}$$

where $\langle \Delta\omega^2 \rangle = \frac{1}{10} \gamma_e^4 \mathbf{h}^2 S(S+1) n \sum\sum \left(1 - 3\cos^2\theta\right)^2 r^{-6}$ is the averaged constant of the spin dipole interaction in a powder-like sample, γ_e is the hyromagnetic ratio for electron, $\mathbf{h} = h/2\pi$ is the Planck constant, $n = n_1 + n_2/\sqrt{2}$, n_1 and n_2 are the concentration of mobile and localized spins, respectively, θ is the angle between the external magnetic field $\mathbf{B}_0$ and spin precession direction, *r* is a minimal distance between spins, $J(\omega_e) = (2\omega_e D_{1D})^{-1/2}$ at $D_{3D} \le \omega_e \le D_{1D}$ and

$J(\omega_e) = (2\omega_e D_{1D})^{-1/2}$ at $\omega_e \leq D_{3D}$ [108]. Assuming spin situation near the units of the cubic lattice with concentration of the monomer units N_c and constant $r_0 = (8/3N_c)^{-1/3}$, the above sum can be simplified as $\sum\sum\left(1-3\cos^2 q\right)^2 r^{-6} = 6.8\, r_0^{-6}$ [109].

The temperature dependences of the effective dynamic parameters D_{1D} and D_{3D} calculated for both types of PC in several PANI samples from the data presented in Fig.3 using Eqs.(8) and (9) are presented in Fig.4. It seems to be justified that the anisotropy of the spin dynamics is maximum in the initial PANI sample, and decreases as y increases.

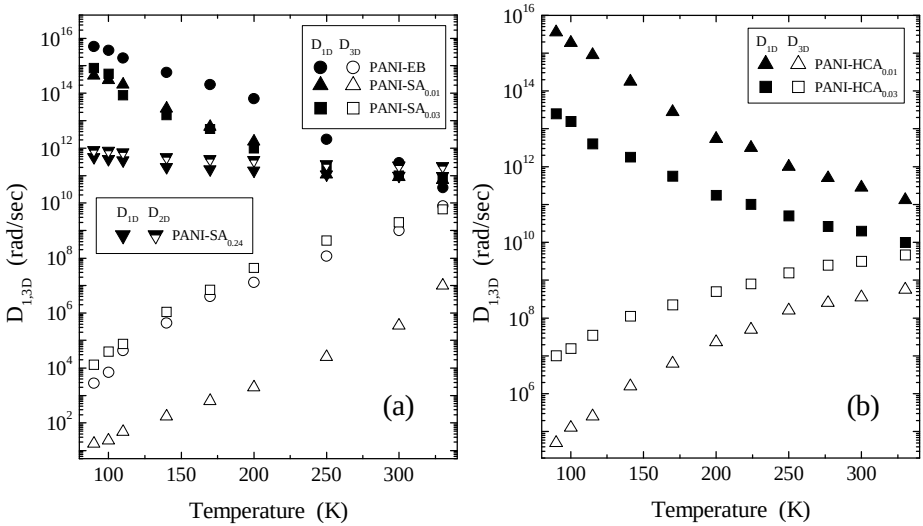

Figure 4. Temperature dependences of effective coefficients of the intrachain and interchain polaron diffusion in undoped, PANI-EB as well as in PANI-SA (*a*) and PANI-HCA (*b*) samples with different doping levels.

At $\omega_e/2\pi \leq 10$ GHz was found [56], that the high anisotropy of the spin dynamics is retained in PANI-HCA with $y = 0.6$ even at room temperature. However, our experimental data indicate that the anisotropy of the motion of the charge carriers is high only in PANI-HCA and PANI-SA with $y < 0.21$. Such a discrepancy is likely due to the limitations appearing at the study of spin dynamics at low frequencies. At $y \geq 0.21$ the system dimensionality seems to grow in PANI-ES, and at high temperatures the spin motion tends to become almost isotropic. The increase in the dimensionality at the polymer doping is accompanied by a decrease in the number of electron traps, which reduces the probability of electron scattering by

the lattice phonons and results in the virtually isotropic spin motion and relatively slight temperature dependences of both the electronic relaxation and diffusion rates of PC, as is the case for amorphous inorganic semiconductors [110,111].

The conductivity of a conducting polymer due to dynamics of N spin charge carriers can be calculated from the modified Einstein relation

$$\sigma_{1,3D}(T) = Ne^2\mu = \frac{Ne^2 D_{1,3D} d_{1,3D}^2}{k_B T}, \qquad (10)$$

where e is elemental charge, μ is the charge carrier mobility, $d_{1,3D}$ are the intrachain, c, and interchain, b, lattice constants summarized in Table 1, and k_B is the Boltzmann constant.

By assuming that the diffusion coefficients D of spin and diamagnetic charge carriers have the same values, one can obtain from Eq.(10) $\sigma_{1D} = 0.1$ S/cm and $\sigma_{3D} = 1 \cdot 10^{-5} - 5 \cdot 10^{-3}$ S/cm at room temperature for the PANI-HCA sample with $0 < y < 0.03$. At $D_{1D} = D_{3D}$, these values were determined to be $\sigma_{1D} = 50 - 180$ and $\sigma_{3D} = 30 - 100$ S/cm. Thus, the conclusion can be drawn, that σ_{3D} grows more strongly with y that is the evidence for the growth of a number and a size of 3D quasi-metal domains in PANI-ES.

Let us consider the charge transfer mechanisms in the initial and slightly doped PANI samples. The fact that the spin-lattice relaxation time of PANI is strongly dependent on the temperature (see Fig.3) means that, in accord with the energy conservation law, electron hops should be accompanied by the absorption or emission of a minimum number of lattice phonons. Multiphonon processes become predominant in neutral PANI because of a strong spin-lattice interaction. For this reason, an electronic dynamics process occurring in the polymer should be considered in the framework of Kivelson's formalism [112-114] of isoenergetic electron transfer between the polymer chains involving optical phonons, because spin and spineless charge carriers probably exist even in an undoped polymer (see Fig.2). In the frames of this model charged spin charge carriers are coulombically bound to charged impurity sites. The excess charge on the carrier site makes a phonon-assisted transition to a neutral carrier moving along another chain. The temperature dependency of the conductivity is then defined by the probability of that the neutral charge carrier is located near the charged impurity and its initial and the final energies are within $k_B T$, hence *ac* conductivity can be determined as [114]

$$\sigma_{ac}(T) = \frac{N_i^2 e^2 \langle y \rangle \xi_{\parallel}^3 \xi_{\perp}^2 \omega_e}{384 k_B T} \left[\ln \frac{2\omega_e L}{\langle y \rangle \gamma(T)} \right]^4 = \frac{\sigma_0 \omega_e}{T} \left[\ln \frac{k_3 \omega_e}{T^{n+1}} \right]^4, \quad (11)$$

where k_1 = 0.45, k_2 = 1.39 and k_3 are constants, $\gamma(T) = \gamma_0(T/300\ \mathrm{K})^{n+1}$ is the transition rate of a charge between neutral and charged carrier states, $\langle y \rangle = y_n y_{ch}(y_n + y_{ch})^{-2}$, y_n, and y_{ch} are respectively the concentrations of neutral and charged carriers per monomer unit, $R_0 = (4\pi N_i/3)^{-1/3}$ is the typical separation between impurities which concentration is N_i; $\xi = (\xi_{\parallel}\xi_{\perp}^2)^{1/3}$, $\xi_{\parallel}$, and $\xi_{\perp}$ are dimensionally averaged, parallel and perpendicular decay lengths for a charge carrier, respectively; L is a number of monomer units per a polymer chain. In this case a weak coupling of the charge with the polymer lattice is realized when hops between the states of a large radius take place.

Figure 5 shows that the experimental data for σ_{1D} of the initial PANI sample is fitted well by Eq.(11) with $\sigma_0 = 2.7 \cdot 10^{-10}$ S K s cm^{-1}, $k_3 = 3.1 \cdot 10^{12}$ s K$^{9.5}$, and n = 8.5. In contrast to undoped *trans*-PA, some quantity of charged carriers exist even in the initial, PANI-EB sample, so the above Kivelson mechanism can determine its conductivity. Such an approach is not evident for PANI doped up to $0.01 \le y \le 0.03$ with less strong temperature dependence. The model of charge carrier scattering on optical phonons of the lattice of metal-like domains described above seems to be more convenient for the explanation of the behavior of their conductivity.

The concentration of mobile spins in PANI-HCA$_{0.01}$ sample is $y_p = 6.1 \cdot 10^{-5}$ per one benzoid ring. Taking into account that each bipolaron possesses dual charge, $y_{bp} = 1.2 \cdot 10^{-3}$ and $\langle y \rangle = 2.3 \cdot 10^{-2}$ can be obtained. The concentration of impurity is $N_i = 2.0 \cdot 10^{19}$ cm^{-3}, so then the separation between them $R_0 = (4\pi N_i/3)^{-1/3} = 2.28$ nm is obtained for this polymer. The prefactor γ_0 in Eq.(11) was determined to be $3.5 \cdot 10^{19}$ Hz. Assuming spin delocalization over five polaron sites [115] along the polymer chain, $\xi_{\parallel} = 1.19$ nm is obtained as well. The decay length of a carrier wave function perpendicular to the chain can be determined from the relation [112,113]

$$\zeta_{\perp} = \frac{b}{\ln(\Delta_0 / t_{\perp})}, \quad (12)$$

where $2\Delta_0$ is the band gap, b is the lattice constant, and $t_{\perp}$ is the hopping matrix element estimated as [116]

$$t_{\perp}^2 = \frac{\mathbf{h}^4 \omega_{ph}^3 D_{3D}}{2\pi E_p} \exp\left(\frac{2E_p}{\mathbf{h}\omega_{ph}}\right), \quad (13)$$

where $\omega_{ph} = 2\pi\nu_{ph}$ is the phonon frequency and E_p is the polaron formation energy. Using $2\Delta_0 = 3.8$ eV [117] typical for π-conjugated polymers $E_p \approx 0.1$ eV [116], $D_{3D} = 3.6 \cdot 10^8$ rad/s determined for PANI-HCA$_{0.01}$, $t_{\perp} = 7.1 \cdot 10^{-3}$ eV, $\xi_{\perp} = 0.079$ nm and $\xi = 0.20$ nm are obtained for this sample. The similar procedure gives $\langle y \rangle = 7.9 \cdot 10^{-2}$, $\gamma_0 = 2.1 \cdot 10^{17}$ sec^{-1}, $\xi_{\perp} = 0.087$ nm. and $\xi = 0.21$ nm for PANI-HCA$_{0.03}$ sample with $y_p = 1.1 \cdot 10^{-3}$ and $y_{bp} = 1.2 \cdot 10^{-2}$.

Temperature dependences of the PANI-SA$_{0.01}$ and PANI-SA$_{0.03}$ samples can be explained in terms of the Kivelson and Heeger model [45] of the charge carrier scattering on the lattice optical phonons in metal-like clusters embedded into polymer matrix. In the framework of this model the total conductivity of the polymers can be expressed in the form [45,118]

$$s_{ac}(T) = \frac{Ne^2 d_{1D}^2 M t_0^2 k_B T}{8p\mathbf{h}^3 a^2} \left[\sinh\left(\frac{E_{ph}}{k_B T}\right) - 1\right] = s_0 T \left[\sinh\left(\frac{E_{ph}}{k_B T}\right) - 1\right], \quad (14)$$

where M is the mass of the polymer unit, t_0 is the transfer integral, for the π-electron equal approximately to 2.5 – 3 eV, E_{ph} is the energy of the optical phonons, and α is the constant of electron-phonon interaction. As can be seen in Fig.5, the $\sigma_{1D}(T)$ dependence obtained for these samples is fairly well fitted using Eq.(14) with $E_{ph} = 0.12$ and 0.11 eV, respectively. These values are near to energy (0.19 eV) of the polaron pinning in heavily doped PANI-ES [119].

A comparatively strong temperature dependency obtained for σ_{3D} of the initial sample can probably be described in the frames of the Elliot model of a thermal activation of charge carriers over energetic barrier E_a from widely separated localized states in the gap to close localized states in the valence and conducting bands tails [120]. In this case *ac* term of a total conductivity is defined mainly by a number of charge carriers excited to the band tails, therefore

$$\sigma_{ac}(T) = \sigma_0 T \omega_e^{\gamma} \exp\left(-\frac{E_a}{k_B T}\right), \quad (15)$$

where $0 \le \gamma \le 1$ is a constant reflecting the dimensionality of a system under study and E_a is the energy for activation of charge carrier to extended states. As the doping level increases the dimensionality of the polymer system rises and activation energy of charge transfer decreases. An approximately linear dependency of γ on E_a was registered [121] for some conjugated polymers. At the same time Parneix *et a.l.* [122] showed $\gamma = 1 - \alpha k_B T/E_a$ ($\alpha = 6$, $E_a = 1.1$ eV) dependency for, e.g., lightly doped poly(3-methylthiophene). Therefore, γ value

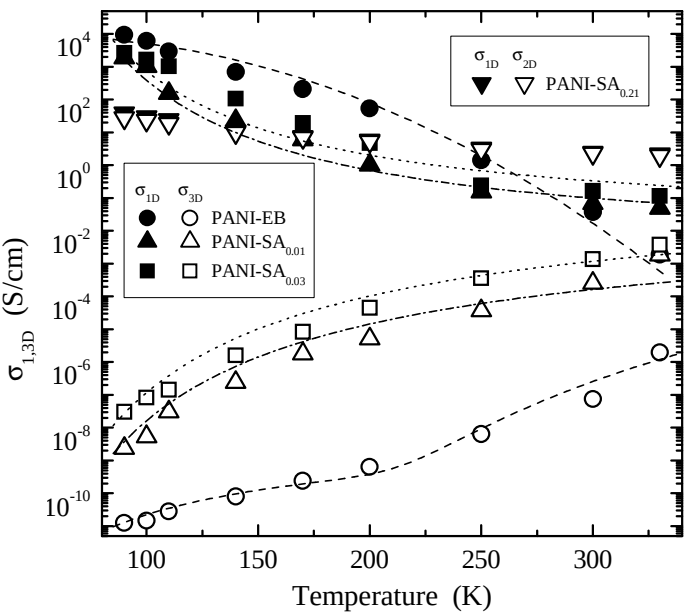

Figure 5. Temperature dependency of the *ac* conductivity due to polaron motion along (σ_{1D}, filled symbols) and between (σ_{3D}, open symbols) polymer chains in the PANI-EB and slightly doped PANI-SA samples as well as an effective rate of spin diffusion in PANI-$SA_{0.21}$ calculated, respectively, in the framework of Q1D (closed symbols) and Q2D (semi-filled symbols) spin transport. The lines show the dependence calculated from Eq.(11) with $\sigma_0 = 2.7 \cdot 10^{-10}$ S K^{-1}s cm^{-1}, $k_3 = 3.1 \cdot 10^{12}$ s $K^{-9.5}$, and $n = 8.5$ (upper dashed line), those calculated from Eq.(14) with $\sigma_0 = 3.95 \cdot 10^{-6}$ S cm^{-1} K^{-1} and $E_{ph} = 0.12$ eV (upper dash-dotted line), $\sigma_0 = 1.75 \cdot 10^{-6}$ S cm^{-1} K^{-1} and $E_{ph} = 0.11$ eV (upper dotted line), and those calculated from Eq.(15) with $\sigma_0 = 8.2 \cdot 10^{-21}$ S $K^{-1}s^{0.8}cm^{-1}$ and $E_a = 0.033$ eV (low temperature region) and $\sigma_0 = 3.9 \cdot 10^{-12}$ S $K^{-1}s^{0.8}cm^{-1}$ and $E_a = 0.41$ eV (high temperature region) (lower dashed line), $\sigma_0 = 4.5 \cdot 10^{-14}$ S $K^{-1}s^{0.8}cm^{-1}$ and $E_a = 0.102$ eV (lower dash-dotted line), $\sigma_0 = 3.1 \cdot 10^{-13}$ S $K^{-1}s^{0.8}cm^{-1}$ and $E_a = 0.103$ eV (lower dotted line).

can be varied in 0.3 – 0.8 range and it reflects the dimensionality of a system under study. As it is seen from Fig.5, Eq.(15) well fits $\sigma_{3D}(T)$ dependence with E_a

equal to 0.033 and 0.41 eV for low- and high-temperature regions, respectively. The activation energy of interchain charge transfer in slightly doped samples is E_a = 0.102 eV for PANI-$SA_{0.01}$ and E_a = 0.103 eV for PANI-$SA_{0.03}$ (Fig.5).

Note that the spin diffusion coefficients and consequently the conductivities, calculated from the spin relaxation of PANI-ES with y = 0.21, in frameworks of one- and two-dimensional spin diffusion, are near to one another (see Fig. 4 and Fig. 5). This fact can possibly be interpreted as the result of the increase of system dimensionality above the percolation threshold lying near $y \approx 0.1$. However, this can be also due to the decrease in accuracy of the saturation method at high doping levels. In this case the dynamics parameters of both spin and spineless charge carriers can be evaluated from the Dyson-like EPR spectrum of PANI with $y \geq 0.21$ using the method described below.

Figure 6 shows the dependency of line width of the PANI-SA on the temperature and doping level. The predominance of extremal $\Delta B_{pp}(T)$ curves evidences for the dipole-dipole exchange interaction of mobile PC with other spins in Q1D polymer system resulting in its effective EPR spectrum broadening. The collision of these PC should to broad EPR spectrum as [72,123]

$$\delta(\Delta B_{pp}) = p\omega_{hop}C_g = k\omega_{hop}C_g\left(\frac{\alpha^2}{1+\alpha^2}\right), \qquad (16)$$

where p is the flip-flip probability during a collision of both spins, ω_{hop} is the frequency of the polaron hopping along a polymer chain, C_g is the number of guest PC per each aniline ring, k = 0.5 for S = 1/2, $\alpha = (3/2)2\pi J_{ex}/\mathbf{h}\,\omega_{hop}$, and J_{ex} is a constant of spin exchange interaction. If the ratio $J_{ex}/\mathbf{h}$ exceeds the frequency of collision of both types of spins, the condition of strong interaction is realized in the system leading to a direct relation of spin-spin interaction and polaron diffusion frequencies, so then lim(p) = 1/2. In the opposite case lim(p) = 9/2 $(\pi/\mathbf{h})^2(J_{ex}/\omega_{hop})^2$. According to the spin exchange fundamental concepts [123] the extremal character of the $\delta(\Delta\omega)(T)$ dependency should evidence the realization of both types of spin-spin interaction respectively at $T \leq T_c$ and $T \geq T_c$. An additional reason of the line broadening can be spin localization with the temperature decrease at $T \geq T_c$. The reason of such exchange can be an interaction of PC localized on neighboring polymer chains modulated by macromolecular librations. Assuming activation character of spin-spin interaction with activation energy E_a, when $\omega_{hop} = \omega_{hop}^0 \exp(-E_a/k_BT)$, one can write for effective line width

$$\Delta B_{pp}(T) = \Delta B_{pp}^{0} + \frac{kC_g\omega_{hop}^{0}\exp(-E_a/k_BT)}{\gamma_e\left[1+\left(\frac{\hbar\omega_{hop}^{0}\exp(-E_a/k_BT)}{3\pi J_{ex}}\right)^2\right]}. \quad (17)$$

Table 2. The ΔB_{pp}^{0} (in G), ω_{hop}^{0} (in 10^{16} rad/s), E_a (in eV), J_{ex}(in eV) parameters calculated from Eq.(17), and the c_P (in emu/mol one ring), $n(e_F)$ (in states/eV one ring), C (in emu K/mol one ring), k_1 (in emu K/mol one ring), and J_{af} (in eV) values determined from Eq.(18) for different PANI samples.

Polymer	ΔB_{pp}^{0}	ω_{hop}^{0}	E_a	J_{ex}	χ_P	$n(\varepsilon_F)$	C	k_1	J_{af}
PANI-SA$_{0.21}$ [a]	4.5	0.75	0.021	0.72					
PANI-SA$_{0.21}$ [b]	4.6	0.96	0.018	0.19	$3.1\cdot10^{-5}$	0.65	$1.2\cdot10^{-2}$	4.2	0.051
PANI-SA$_{0.42}$ [a]	3.1	17	0.051	0.64					
PANI-SA$_{0.42}$ [b]	2.7	5.1	0.021	0.59		0.90			
PANI-SA$_{0.53}$ [a]	2.5	17	0.052	0.49					
PANI-SA$_{0.53}$ [b]	2.4	93	0.024	0.66	$1.4\cdot10^{-3}$	1.4	$1.6\cdot10^{-2}$	48.6	0.057
PANI-HCA$_{0.50}$						1.9			
PANI-AMPSA$_{0.4}$ [a,c]					$9.8\cdot10^{-7}$		$4.5\cdot10^{-4}$	$1.5\cdot10^{-2}$	0.001
PANI-AMPSA$_{0.4}$ [a,d]					$1.1\cdot10^{-4}$	0.42	$7.2\cdot10^{-3}$	$1.1\cdot10^{-2}$	0.005
PANI-AMPSA$_{0.6}$ [a,c]					$2.2\cdot10^{-5}$		$1.7\cdot10^{-2}$	$1.7\cdot10^{-2}$	0.004
PANI-AMPSA$_{0.6}$ [a,d]					$5.3\cdot10^{-3}$	3.5	$6.5\cdot10^{-1}$	$1.2\cdot10^{-2}$	0.006
PANI-CSA$_{0.5}$ [a,c]					$5.2\cdot10^{-7}$		$2.3\cdot10^{-4}$	$9.1\cdot10^{-3}$	0.005
PANI-CSA$_{0.5}$ [a,d]					$2.7\cdot10^{-4}$	1.2	$2.7\cdot10^{-2}$	1.58	0.004
PANI-CSA$_{0.6}$ [a,c]					$8.5\cdot10^{-7}$		$4.2\cdot10^{-4}$	$6.6\cdot10^{-3}$	0.014
PANI-CSA$_{0.6}$ [a,d]					$7.1\cdot10^{-5}$	1.8	$2.2\cdot10^{-2}$	2.13	0.004
PANI-*p*TSA$_{0.5}$ [a,e]					$7.9\cdot10^{-6}$	0.6	$1.3\cdot10^{-3}$	1.44	0.099
PANI-*p*TSA$_{0.5}$ [b,e]					$3.3\cdot10^{-6}$	0.12	$1.1\cdot10^{-3}$	0.29	0.041
PANI-*p*TSA$_{0.5}$ [a,f]	12.2	$1.3\cdot10^{19}$	0.102	0.36		9.1			
PANI-*p*TSA$_{0.5}$ [b,f]	1.7	$9.6\cdot10^{17}$	0.058	0.28	$5.6\cdot10^{-4}$	27	$3.9\cdot10^{-2}$		

Notes: [a] determined at 3-cm waveband EPR, [b] determined at 2-mm waveband EPR, [c] determined for PC R_1, [d] determined for PC R_2, [e] in nitrogen atmosphere, [f] in air atmosphere.

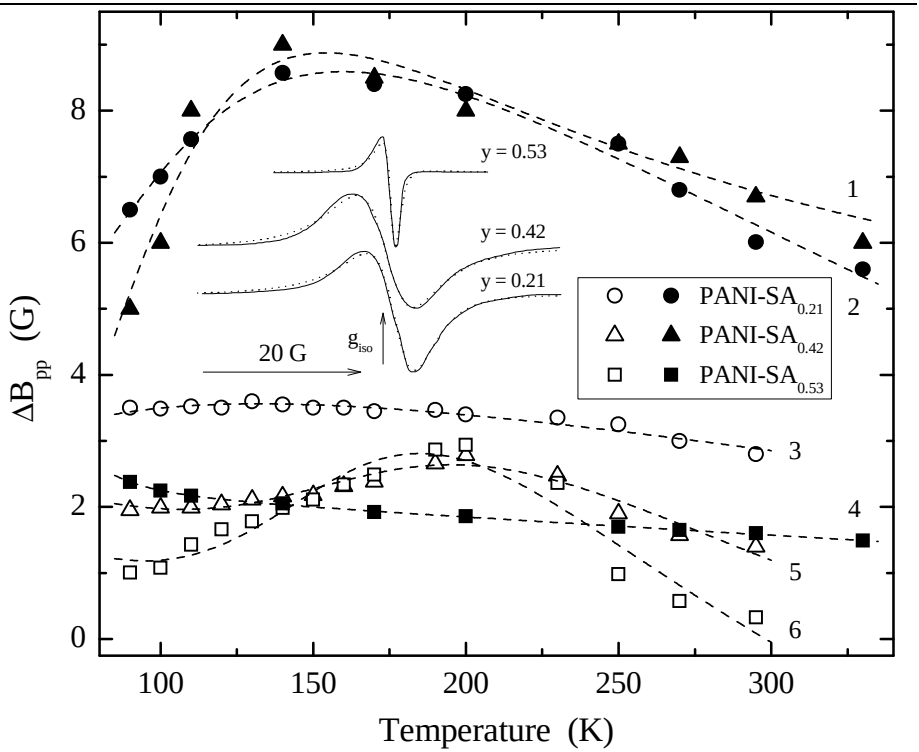

Figure 6. Temperature dependence of line width of PC in PANI-SA with different doping levels registered at 3-cm (open points) and 2-mm (filled points) wavebands. The dependences calculated from Eq.(17) with ω_{hop}^{0} = 5.1·10^{16} s^{-1}, E_a = 0.021 eV, J_{ex} = 0.59 eV (*1*), ω_{hop}^{0} = 9.5·10^{15} s^{-1}, E_a = 0.018 eV, J_{ex}= 0.19 eV (*2*), ω_{hop}^{0} = 7.5·10^{15} s^{-1}, E_a = 0.021 eV, J_{ex}= 0.72 eV (*3*), ω_{hop}^{0} = 9.3·10^{17} s^{-1}, E_a = 0.024 eV, J_{ex}= 0.66 eV (*4*), ω_{hop}^{0} = 1.7·10^{17} s^{-1}, E_a = 0.051 eV, J_{ex}= 0.64 eV (*5*), and ω_{hop}^{0} = 1.9·10^{17} s^{-1}, E_a = 0.052 eV, J_{ex}= 0.49 eV (*6*) are shown by dashed lines. Insert – RT 2-mm waveband absorption spectra of PC in PANI-SA with different doping levels. Top-down dotted lines present the spectra calculated from Eq.(19), Eq.(22), and (23) with respective D/A = 0.895, ΔB_{pp} = 1.48 G, D/A = 0.16, ΔB_{pp} = 7.10 G, and D/A =0.53, ΔB_{pp} = 5.86 G.

Figure 6 indicates good applicability of this approach to the interpretation of the PANI-SA line width. The appropriate parameters calculated from Eq.(17) are summarized in Table 2. The activation energy of spin-spin interaction E_a decreases at the increase of polarizing magnetic field and lies near activation energy of the macromolecular librations (0.015 eV) determined above. This is an

evidence of the dependency of the spin-spin interaction on an external magnetic field and its correlation with macromolecular dynamics in the system. The $\Delta B_{pp}(T)$ dependences presented evidence also of different charge transport mechanisms in this polymer with different doping levels. The mechanism affecting the line width, however, depends also on the electron precession frequency, so then the line width does not directly reflects the relaxation and dynamics parameters of PC in this polymer.

The *g*-factor of PC R_2 in PANI-SA with $y \geq 0.21$ becomes isotropic and decreases from $g_{R2} = 2.0041_8$ down to $g_{iso} = 2.0031_4$. This is accompanied by a narrowing of the R_2 line (Fig.6). Such effects can be explained by a further depinning of Q1D spin diffusion along the polymer chain, and therefore spin delocalization, and by the formation of areas with high spin density in which a strong exchange of spins on neighboring chains occurs. This is in agreement with the supposition [27,30,38-41] of formation in amorphous PANI-EB of high-conductive massive domains with 3D delocalized electrons.

The doping of the PANI with sulphuric acid leads to an inverted Λ-like temperature dependence of an effective paramagnetic susceptibility (see Fig.7), as occurs in the case of polyaniline perchlorate [75]. However, this does not lead to a strong narrowing of the PC line (Fig.6). As in the case of ***e.g.*** PANI treated with ammonia, this should indicate a strong antiferromagnetic spin interaction due to a singlet-triplet equilibrium in the PANI-SA between N spins with $S = ½$. This should lead to appearance in the total paramagnetic susceptibility χ except the Pauli susceptibility of the Fermi gas χ_P also of a temperature-dependent contributions of localized Curie PC χ_C and the term χ_{ST} coming due to a possible singlet-triplet spin equilibrium in the system [124,125],

$$\chi = \chi_P + \chi_C + \chi_{ST} = N_A \mu_{eff}^2 n(\varepsilon_F) + \frac{N\mu_{eff}^2}{3k_B T} + \frac{k_1}{T}\left[\frac{\exp(-J_{af}/k_B T)}{1+3\exp(-J_{af}/k_B T)}\right]^2 \quad (18)$$

where N_A is the Avogadro's number, $\mu_{eff} = \mu_B g\sqrt{S(S+1)}$ is the effective magneton, μ_B is the Bohr magneton, $N\mu_{eff}^2/3k_B = C$ is the Curie constant per mole-C/mol-monomer, k_1 is a constant, and J_{af} is the antiferromagnetic exchange coupling constant. The contributions of the χ_c and χ_p terms to the total paramagnetic susceptibility depend on various factors, for example, on the nature and mobility of charge carriers can vary at the system modification.

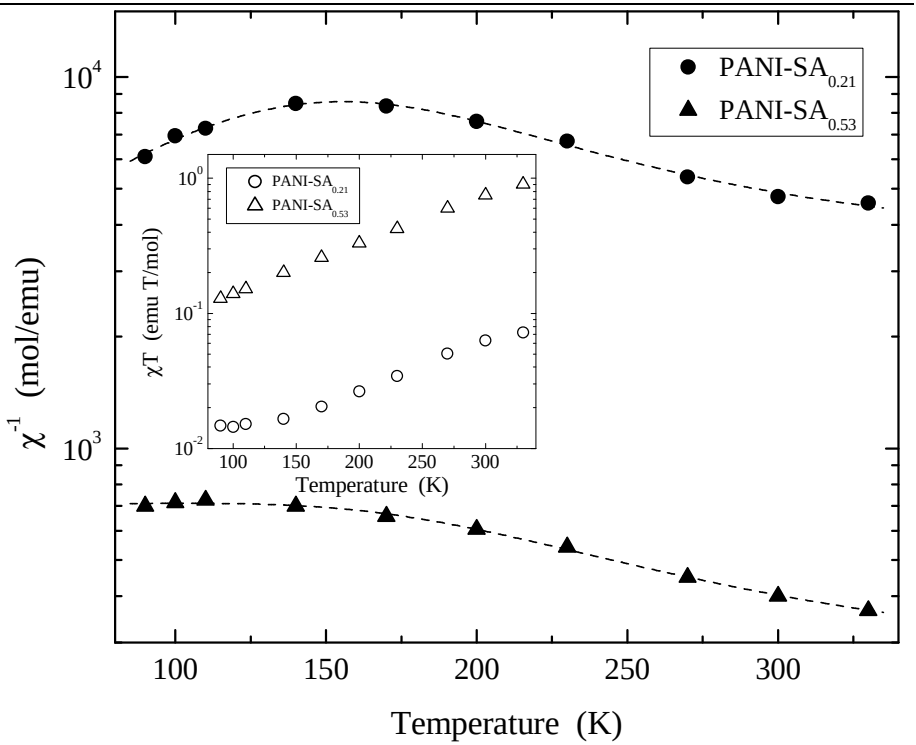

Figure 7. Temperature dependence of inversed paramagnetic susceptibility and χT product (insert) of PANI-SA samples with different doping levels. Above and lower dashed lines show the dependences calculated from Eq.(18) with respective $\chi_P = 3.1 \cdot 10^{-5}$ emu/mol, $C = 1.2 \cdot 10^{-2}$ emu K/mol, $k_1 = 4.2$ emu K/mol, $J_{af} = 0.051$ eV, and $\chi_P = 1.4 \cdot 10^{-3}$ emu/mol, $C = 1.6 \cdot 10^{-2}$ emu K/mol, $k_1 = 48.6$ emu K/mol, $J_{af} = 0.057$ eV.

Indeed, Fig.7 shows that the paramagnetic susceptibility experimentally determined for the PANI-SA samples is well reproduced by Eq.(18) with the parameters also presented in Table 2. The J_{af} value is close to that (0.078 eV) obtained for the ammonia treated PANI [75]. Note that $n(\varepsilon_F)$ determined for PANI-SA, consistent with those determined earlier for PANI heavily doped with other counterions [11,21,126]. With the assumption of a metallic behavior one can estimate that the energy of N_P Pauli spins in *e.g.* PANI-ES, with $0.21 \le y \le 0.53$, $\varepsilon_F = 3N_p/2n(\varepsilon_F)$ [110] is to be 0.1 – 0.51 eV [86]. This value is near to that (0.4 eV) obtained, *e.g.*, for PANI-CSA [20]. From this value the number of charge carriers with mass $m_c = m_e$ in heavily doped PANI-SA [110], $N_c = (2m_c\varepsilon_F/\mathbf{h}^2)^{3/2}/3\pi^2 \approx 1.7 \cdot 10^{21}$ cm^{-3} is evaluated. The N_c value is close to a total spin concentration in PANI-SA. This fact leads to the conclusion that all PC take

part in the polymer conductivity. For heavily doped PANI-SA samples, the concentration of spin charge carriers is less than that of spineless ones, due to the possible collapse of pairs of polarons into diamagnetic bipolarons. The velocity of the charge carrier near the Fermi level can be calculated [110], as $v_F = 2d_{1D}/\pi\hbar n(\varepsilon_F) = (3.3 - 7.2)\cdot 10^7$ cm/s typical for other conducting polymers [49,79].

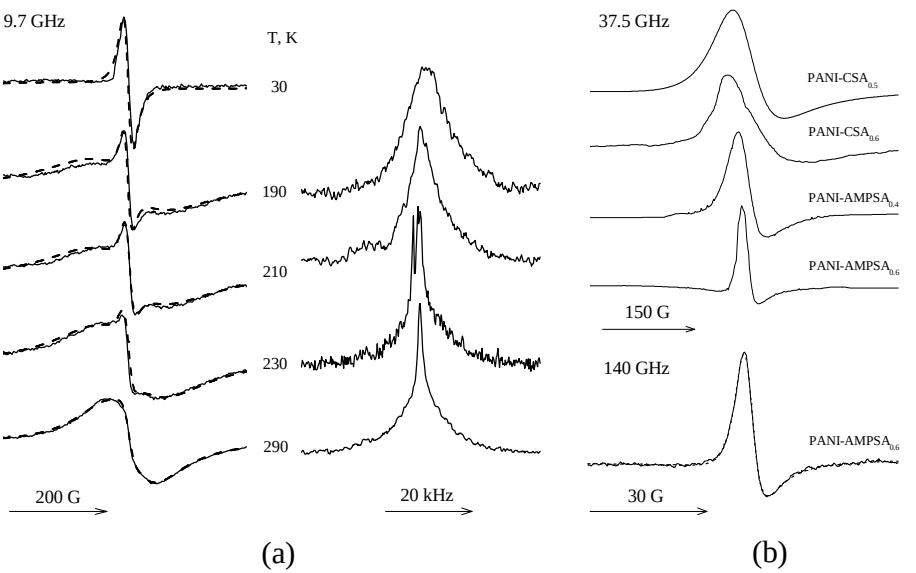

Figure 8. (*a*) 3-cm waveband EPR (left) and 400 MHz ^{1}H NMR (right) spectra of PANI-$CSA_{0.5}$ sample registered at different temperatures. Top-down dashed lines show sum of two spectra each calculated from Eq.(19), Eq.(20), and (21) with respective $D_1/A_1 = 0.041$, $\Delta B_{pp1} = 19.9$ G, $D_2/A_2 = 0.034$, $\Delta B_{pp2} = 492$ G; $D_1/A_1 = 0.12$, $\Delta B_{pp1} = 18.1$ G, $D_2/A_2 = 0.042$, $\Delta B_{pp2} = 173$ G; $D_1/A_1 = 0.31$, $\Delta B_{pp1} = 21.7$ G, $D_2/A_2 = 0.04$, $\Delta B_{pp2} = 172$ G; $D_1/A_1 = 0.34$, $\Delta B_{pp1} = 24.1$ G, $D_2/A_2 = 0.03$, $\Delta B_{pp2} = 152$ G; $D_1/A_1 = 0.26$, $\Delta B_{pp1} = 28.4$ G, $D_2/A_2 = 0.02$, $\Delta B_{pp2} = 111$ G. (*b*) RT 8-mm and 2-mm waveband EPR spectra of PANI-CSA and PANI-AMPSA with different doping levels. The spectrum calculated with $D/A = 1.30$ and $\Delta B_{pp} = 5.33$ G is shown as well.

The shape of EPR spectrum of PANI-ES depends on the nature of counterion. Figure 8 presents EPR spectra of highly doped film-like PANI-CSA and PANI-AMPSA samples registered at different polarizing frequencies. For the comparison, NMR spectra of PANI-$CSA_{0.5}$ registered at different temperatures are presented as well. These spectra were analyzed to contain Dysonian contribution [73] due to interaction of the exciting MW field with charge carriers in the material bulk. This leads to the appearance of the skin-layer on the sample

surface. When the thickness of skin-layers δ becomes comparable or thinner than a characteristic size of a sample, *e.g.* due to the increase of intrinsic conductivity σ_{ac}, the time of charge carrier diffusion through the skin-layer becomes essentially less than a spin relaxation time and the Dysonian line with characteristic asymmetry factor *A*/*B* (the ratio of intensities of the spectral positive peak to negative one) is registered as it is shown in the insert of the Fig.6. Such line shape distortion is registered in EPR spectra of highly-doped PANI and other conjugated polymers [47-49,103,127].

Generally, first derivative of the Dysonian line consists of absorption and dispersion terms,

$$\frac{d\chi}{dB} = A\frac{2x}{(1+x^2)^2} + D\frac{1-x^2}{(1+x^2)^2} \tag{19}$$

where $x = 2(B\text{-}B_0) / \sqrt{3}\Delta B_{pp}^{L}$. If a skin-layer is formed on a surface of polymer plate with a thickness of 2*d* the coefficients *A* and *D* can be determined from relations [128]

$$A = \frac{\sinh p + \sin p}{2p\ (\cosh p + \cos p)} + \frac{1+\cosh p\ \ \cos p}{(\cosh p + \cos p)^2}, \tag{20}$$

$$D = \frac{\sinh p - \sin p}{2p\ (\cosh p + \cos p)} + \frac{\sinh p\ \ \sin p}{(\cosh p + \cos p)^2}, \tag{21}$$

where $p = 2d/\delta$, $\delta = \sqrt{2/\mu_0\omega_e\sigma_{ac}}$, and μ_0 is the magnetic permeability for vacuum. From the analysis it was determined that the line asymmetry parameter *A*/*B* is correlated with the coefficients *A* and *D* of Eq.(19) simply as *A*/*B* = 1 + 1.5 *D*/*A* independently on the EPR signal line width. Thus, it appears to be possible to determine correctly line width, magnetic susceptibility, *g*-factor of PC with Dysonian EPR spectra shown above. Konkin *et al.* shown [85] that in case of PANI-CSA and PANI-AMPSA the Dysonian line asymmetry factor *A*/*B* and therefore the ratio *D*/*A* depend more complicated on the 2*d*/δ ratio in Eq.(20) and Eq.(21). The *D*/*A*(2*d*/δ) dependences calculated for these polymer presented in Fig.9. It was shown the applicability of these functions for the analysis of Dysonian EPR spectra of PC in an initial and also in two, three and four times

incrassate PANI films (Fig.9). Such procedure allows determining intrinsic conductivity σ_{ac} of both the highly doped film-like PANI-CSA and PANI-AMPSA samples directly from their Dysonian spectrum.

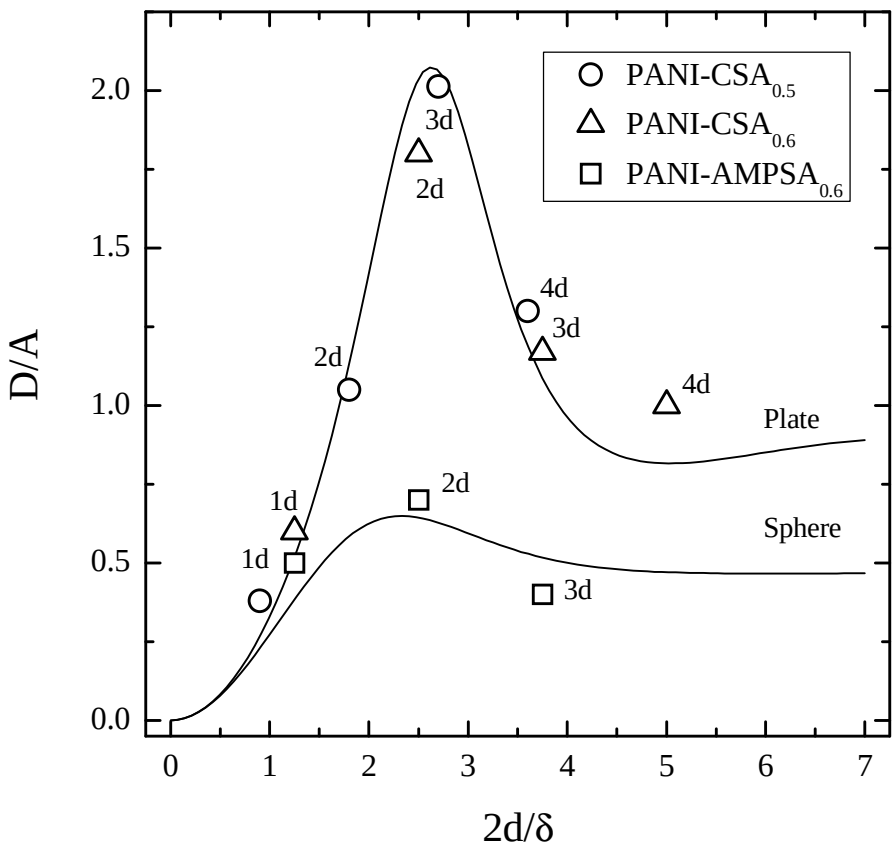

Figure 9. The theoretical $D/A(2d/\delta)$ dependencies calculated [85] and experimentally determined for the PAN-CSA and PAN-AMPSA films with different plate thickness (*nd*) at 3-cm waveband EPR and 300 K.

EPR spectra of PANI-CSA and PANI-AMPSA were then analyzed as sum of two different spin ensembles coexisting in these polymers with different Dysonian shapes, namely narrow EPR spectrum of PC R_1 with g = 2.0028 localized in amorphous polymer matrix and broader EPR spectrum of PC R_2 with g = 2.0020 and higher mobility in crystalline phase of the polymers. The cooling of the samples leads to the decrease in the relative concentration of PC R_2 and to the monotonous increase in its line width, as it is seen in Fig.8 and Fig.10. In the

same time, the line width of PC R_1 decreases monotonously and the sum spin concentration increases at the temperature decrease. Besides, NMR line width decreases at such a sample cooling (Fig.8) due possible to the decrease of interaction of electron and proton spins. The RT ΔB_{pp} value of PC R_2 in *e.g.* PANI-AMPSA$_{0.6}$ decreases from 54 down to 20 and then down to 5.3 G at the increase of registration frequency $\omega_e/2\pi$ from 9.7 up to 36.7 and then up to 140 GHz (Fig.8), so one can express this value as $\Delta B_{pp}(\omega_e) = 1.5 + 2.2 \cdot 10^9 \omega_e^{-0.84}$ G. Such extrapolation reveals the dependence of spin-spin relaxation time on the registration frequency and allows estimating correct line width at $\omega_e \to 0$ limit to be 1.5 G.

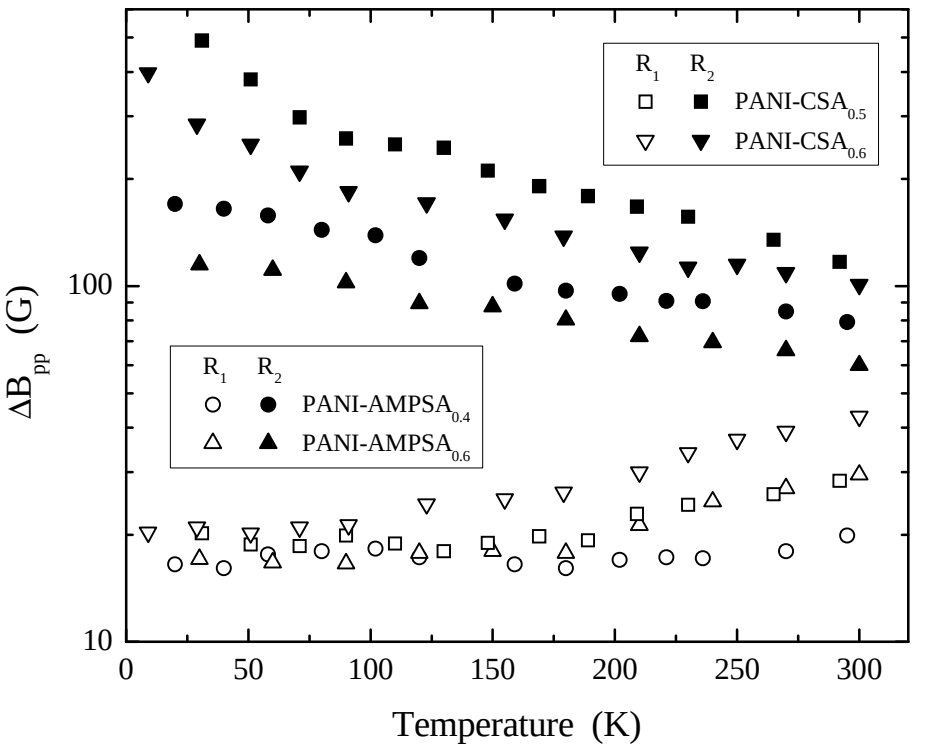

Figure 10. Temperature dependence of line width of PC R_1 and R_2 in PANI-CSA and PANI-AMPSA samples with different doping levels determined from their 3-cm waveband EPR spectra taking into consideration the Dyson contribution.

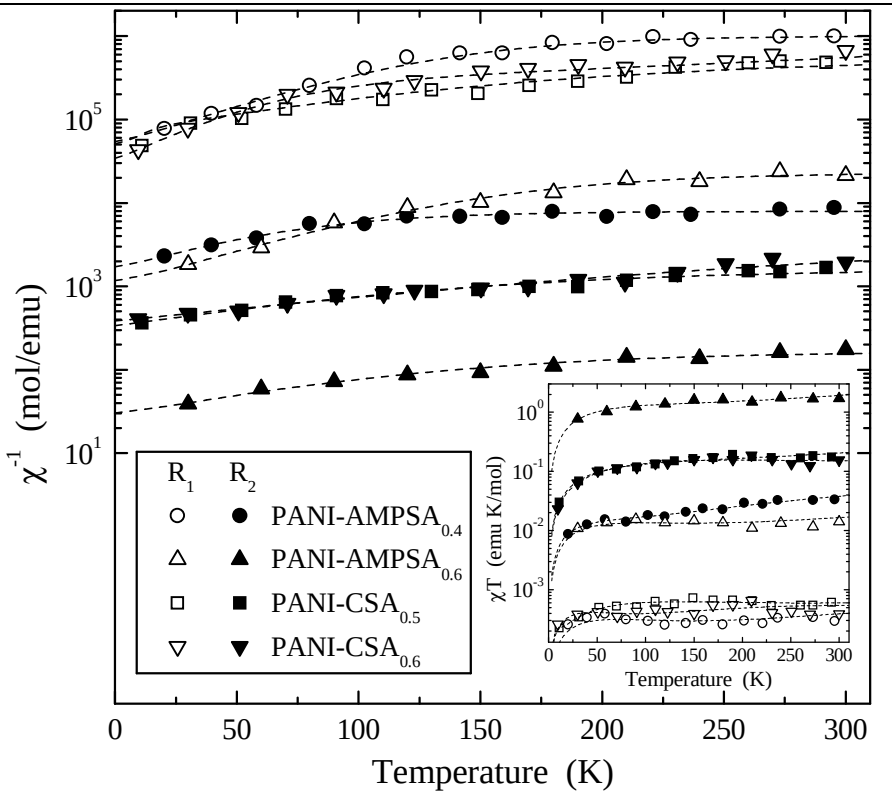

Figure 11. Temperature dependence of inversed effective paramagnetic susceptibility χ and χT product (insert) of PANI-AMPSA and PANI-CSA samples with different doping levels. Top-down dashed lines show the dependences calculated from Eq.(18) with respective $\chi_P = 9.8 \cdot 10^{-7}$ emu/mol, $C = 4.5 \cdot 10^{-4}$ emu K/mol, $k_1 = 1.5 \cdot 10^{-2}$ emu K/mol, $J_{af} =$ 0.001 eV, $\chi_P = 8.5 \cdot 10^{-7}$ emu/mol, $C = 4.2 \cdot 10^{-4}$ emu K/mol, $k_1 = 6.6 \cdot 10^{-3}$ emu K/mol, $J_{af} =$ 0.014 eV, $\chi_P = 5.2 \cdot 10^{-7}$ emu/mol, $C = 2.3 \cdot 10^{-4}$ emu K/mol, $k_1 = 9.1 \cdot 10^{-3}$ emu K/mol, $J_{af} =$ 0.005 eV, $\chi_P = 2.2 \cdot 10^{-5}$ emu/mol, $C = 1.7 \cdot 10^{-2}$ emu K/mol, $k_1 = 1.7 \cdot 10^{-2}$ emu K/mol, $J_{af} =$ 0.004 eV, $\chi_P = 1.1 \cdot 10^{-4}$ emu/mol, $C = 7.2 \cdot 10^{-3}$ emu K/mol, $k_1 = 1.1 \cdot 10^{-2}$ emu K/mol, $J_{af} =$ 0.005 eV, $\chi_P = 7.1 \cdot 10^{-5}$ emu/mol, $C = 2.2 \cdot 10^{-3}$ emu K/mol, $k_1 = 2.13$ emu K/mol, $J_{af} =$ 0.004 eV, $\chi_P = 2.7 \cdot 10^{-4}$ emu/mol, $C = 2.7 \cdot 10^{-2}$ emu K/mol, $k_1 = 1.58$ emu K/mol, $J_{af} =$ 0.004 eV, $\chi_P = 5.3 \cdot 10^{-3}$ emu/mol, $C = 6.5 \cdot 10^{-1}$ emu K/mol, $k_1 = 1.2 \cdot 10^{-2}$ emu K/mol, $J_{af} =$ 0.006 eV.

The narrowing of the line on raising the PANI temperature can be explained by averaging of the local magnetic field caused by HFI between the localized spins whose energy levels lie near the Fermi level. The EPR line of PANI·CSA and PANI-AMPSA may also be broadened to some extent by relaxation due to

the spin-orbital interaction responsible for linear dependence of T_1^{-1} on temperature [53]; however, this interaction seems to be rather weak in our case. It is significant that for both types of PC the line widths are appreciably larger than those obtained previously for the fully oxidized powder-like and film-like PANI·CSA (0.35 and 0.8 G, respectively) [53], which indicates a higher conductivity of the samples under study. Comparison of the ΔB_{pp} values obtained for different PANI·CSA samples [85] suggested that a crystalline phase is formed in the amorphous phase of the polymer, beginning with the oxidation level y = 0.3, and that the paramagnetic centers of this newly formed phase exhibit a broader EPR spectrum. In the amorphous phase of the polymer, the paramagnetic centers of radicals of the R_1 type are characterized by less temperature-dependent line width and are likely not involved in the charge transfer being, however, as probes for whole conductivity of the sample. At the same time, the magnetic resonance parameters of radicals of the R_2 type should reflect the charge transport in the crystalline domains of PANI·CSA and PANI-AMPSA. The line width of PANI appreciably decreases on replacement of the CSA anion by the AMPSA anion (see Fig.10), which is likely due to the shortening of spin-spin relaxation time of both PC.

Figure 11 depicts the effective paramagnetic susceptibility of both the R_1 and R_2 PC as function of temperature. The J_{af} values obtained are much lower of the corresponding energy (0.078 eV) obtained for ammonia-doped PANI [75]. It is seen that at low temperatures when $T \le T_c \approx 100$ K the Pauli and Curie terms prevail in the total paramagnetic susceptibility χ of both type PC in all PANI samples. At $T \ge T_c$, when the energy of phonons becomes comparable with the value $k_B T_c \approx 0.01$ eV, the spins start to interact that causes the appearance of the last term of Eq.(18) in sum susceptibility as result of the equilibrium between the spins with triplet and singlet states in the system. It is evident that the R_1 signal susceptibility obeys mainly the Curie law typical for localized isolated PC, whereas the R_2 susceptibility consists of the Curie-like and Pauli-like contributions.

The $n(\varepsilon_F)$ values obtained for the charge carriers in PANI-CSA and PANI-AMPSA are also summarized in Table 2. This value increases in series PANI-$AMPSA_{0.4}$ → PANI-$CSA_{0.5}$ → PANI-$CSA_{0.6}$ → PANI-$AMPSA_{0.6}$. This density of stated of polarons in PANI-CSA is in agreement with that obtained previously in the optical (0.06—6 eV) [15] and EPR [53] studies of this polymer. The Fermi energy of the Pauli-spins was calculated to be $\varepsilon_F \approx 0.2$ eV. This value is lower than the Fermi energy obtained for highly CSA- (0.4 eV) [20] and sulfur- (0.5 eV) [48,86] doped PANI. Assuming again that the charge carrier mass in heavily

doped polymer is equal to the mass of free electron ($m_c = m_e$), the number of charge carriers in such a quasi-metal [110], $N_c \approx 4.1 \cdot 10^{20}$ cm^{-3} was determined. This is close to the spin concentration in this polymer; therefore, one can conclude that all delocalized PC are involved in the charge transfer in PANI-CSA$_{0.6}$. The velocity of charge carriers near the Fermi v_F level was calculated to be $3.8 \cdot 10^7$ cm/s for PANI-CSA that is close to those evaluated for this polymer from the EPR magnetic susceptibility data, $(2.8 - 4.0) \cdot 10^7$ cm/s [129,130], and $6.2 \cdot 10^7$ cm/s for PANI-AMPSA.

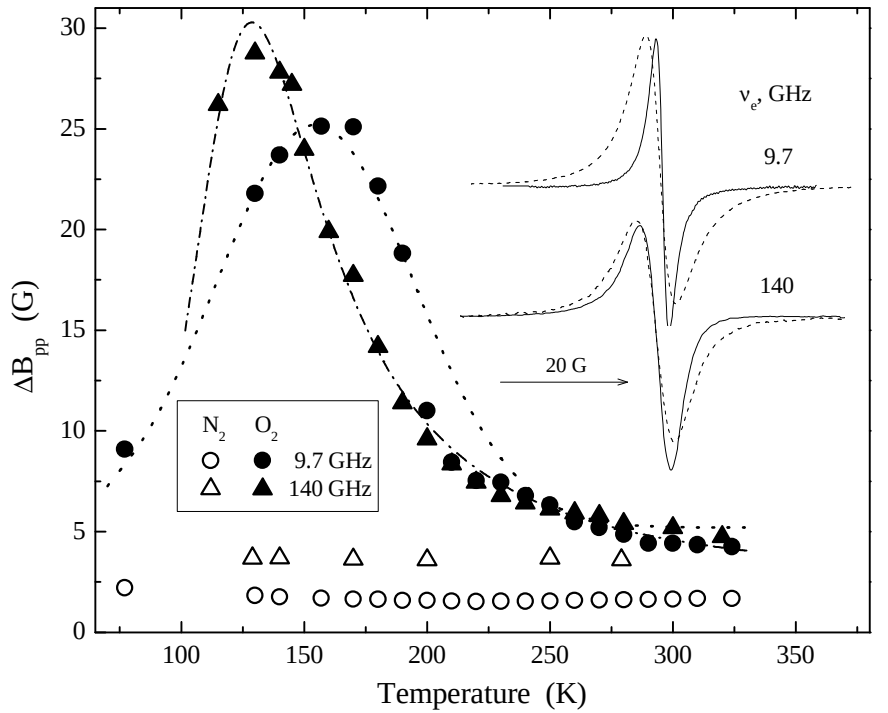

Figure 12. Insert – 3-cm and 2-mm wavebands EPR spectra of the PANI-*p*TSA$_{0.50}$ sample in nitrogen (solid lines) and air (dashed lines) atmosphere. Temperature dependence of line width of PC in the PANI-*p*TSA sample with the presence of nitrogen and oxygen molecules registered at 3-cm and 2-mm wavebands EPR. The lines show the dependences calculated from Eq.(17) with $\omega^0_{hop} = 9.6 \cdot 10^{17}$ s^{-1}, $E_a = 0.058$ eV, $J_{ex} = 0.28$ eV (dash-dotted line), $\omega^0_{hop} = 1.3 \cdot 10^{19}$ s^{-1}, $E_a = 0.102$ eV, $J_{ex} = 0.36$ eV (dotted line).

Thus, main PC in the highly doped PANI·CSA and PANI-AMPSA samples are localized at $T \le T_c$. This is the reason for the Curie type of susceptibility of

the sample and should lead to the VRH charge transfer between the polymer chains. The spin-spin exchange is stimulated at $T \geq T_c$ due likely to the activation librations of the polymer chains. The activation energies of these librations lie within the energy range characteristic of PANI-CSA [131] and PANI-HCA [80,82]. The E_a value depends on the effective rigidity and planarity of the polymer chains that are eventually responsible for the electrodynamic properties of the polymer.

PANI-*p*TSA$_{0.50}$ in nitrogen atmosphere at 3-cm waveband EPR demonstrates Lorentzian exchange-narrowed line which an asymmetry factor *A*/*B* is 1.03 (Fig.12). The exposure of the samples to air was observed to lead to reversible line broadening and an increase in the asymmetry factor up to 1.27. The asymmetry of the EPR line may be due to either unresolved anisotropy of the *g*-factor or the presence in the spectrum of the Dyson term [73] as in case of other highly doped conducting polymers. To verify these assumptions, the 2-mm waveband EPR spectra of the sample were recorded. It is seen from Fig.12 that this polymer in this waveband EPR also exhibits a single asymmetric line, whose asymmetry factor varies at the exposition to air from 1.68 up to 1.95. This fact indicates substantial interaction of PC even in high fields, the line asymmetry of these PC indeed results from the interaction of a MW field with charge carriers in the skin layer. Dysonian EPR spectra of the samples were calculated from Eq.(19) with the following coefficients *A* and *D* for skin-layer on the surface of a spherical powder particle with radius *R* [128]:

$$\frac{4A}{9} = \frac{8}{p^4} - \frac{8\ (\sinh p + \sin p)}{p^3(\cosh p - \cos p)} + \frac{8\ \sinh p\ \sin p}{p^2(\cosh p - \cos p)^2} + \frac{(\sinh p - \sin p)}{p\ (\cosh p - \cos p)} - \frac{(\sinh^2 p - \sin^2 p)}{(\cosh p - \cos p)^2} + 1, \quad (22)$$

$$\frac{4D}{9} = \frac{8\ (\sinh p - \sin p)}{p^3(\cosh p - \cos p)} - \frac{4\ (\sinh^2 p - \sin^2 p)}{p^2(\cosh p - \cos p)^2} + \frac{(\sinh p + \sin p)}{p\ (\cosh p - \cos p)} - \frac{2\sinh p\ \sin p}{(\cosh p - \cos p)^2}, \quad (23)$$

(here $p = 2R/\delta$) and the main magnetic parameters were obtained.

As the operating frequency increases from 9.7 up to 140 GHz, the ΔB_{pp} value of PC in the PANI sample increases not more than by a factor of 2 (Fig.12). Such insignificant line broadening with the operating frequency increase was not observed in studies on other conducting polymers, including PANI. This may be evidence for stronger exchange interaction between PC in the polymers, which is not completely relieved in strong magnetic field. The temperature dependences of the effective absorption line width of this sample determined at both the 3-cm and 2-mm wavebands EPR are presented in Fig.12. It is seen that ΔB_{pp} of PC in the sample containing nitrogen slightly depends on temperature. Air diffusion into the sample leads to the reversible extremal broadening of their EPR line (Fig.12).

At the increase of polarizing frequency from 9.7 GHz up to 140 GHz the characteristic temperature T_c of the $\Delta B_{pp}(T)$ dependences presented shifts from 160 K to 130 K (Fig.12). Such effect was interpreted as result of activation dipole-dipole interaction of polarons with oxygen molecules possessing sum spin S = 1. The $\Delta B_{pp}(T)$ dependences were fitted by Eq.(17) with appropriate parameters listed in Table 2 (Fig.12). It is seen that the experimental data obtained can be rationalized well in terms of this theory. The obtained value of J_{ex} sufficiently exceeds the corresponding spin-exchange constant for nitroxide radicals with paramagnetic ions, $J_{ex} \leq 0.01$ eV [123].

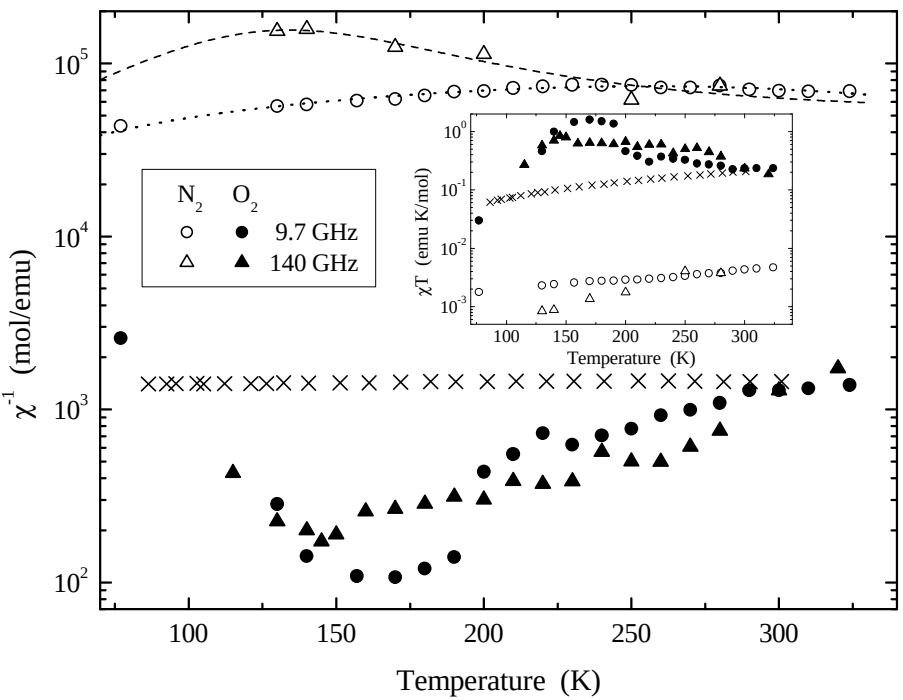

Figure 13. Temperature dependence of inversed effective paramagnetic susceptibility and χT product (insert) of PC in PANI-pTSA$_{0.5}$ exposed to nitrogen (open symbols) and oxygen (filled symbols). By the "×" symbol is shown the appropriate data obtained for this system in [132] by using a "force" magnetometer in a *dc* external magnetic field of $5 \cdot 10^3$ G. Dashed and dotted lines show the dependences calculated from Eq.(18) with respective $\chi_P = 3.3 \cdot 10^{-6}$ emu/mol, $C = 1.1 \cdot 10^{-3}$ emu K/mol, $k_1 = 0.29$ emu K/mol, J_{af} = 0.041 eV and $\chi_P = 7.9 \cdot 10^{-6}$ emu/mol, $C = 1.3 \cdot 10^{-3}$ emu K/mol, $k_1 = 1.44$ emu K/mol, J_{af} = 0.099 eV.

Figure 13 shows the temperature dependence for the paramagnetic susceptibility of PANI-*p*TSA$_{0.50}$ sample in the absence and in the presence of oxygen in the polymer matrix. An analysis of the paramagnetic susceptibility of the nitrogen containing sample determined at 3-cm and 2-mm wavebands EPR showed that it can be described by Eq.(18) with the parameters summarized in Table 2. These data show that the transition of registration frequency from 9.7 GHz to 140 GHz leads to decrease in J_{af} of nitrogen containing PANI-*p*TSA$_{0.5}$ from 0.099 eV down to 0.041 eV due possible to the field effect. The Figure reveals that the effective susceptibility of the PANI-*p*TSA$_{0.50}$ without oxygen, as determined from 3-cm waveband EPR spectra, slightly varies with temperature. However, this quantity determined from the 2-mm waveband EPR spectra noticeably decreases with a decrease in temperature. The exposure of the polymer to air increases proportionally all components of its magnetic susceptibility. This value of the sample exposed to air increases and exhibits non-monotonic temperature dependence in the 3-cm and 2-mm wavebands EPR with a characteristic temperature maximum at 160 and 150 K. This effect is discussed above and attributed to the spin exchange interaction. The Pauli susceptibility of the sample is close to that determined in [17] at $n(\varepsilon_F) = 22.8$ eV^{-1}. Note, that the χ measured for this polymer by more direct method [132] exhibits smaller temperature dependency.

The velocity of charge carriers and the Fermi energy were calculated as $v_F = 2d_{1D}/\pi\hbar\, n(\varepsilon_F)$ and $\varepsilon_F = 3N_e/2n(\varepsilon_F)$ to be $3.1\cdot10^6$ cm/s and 0.16 eV, respectively. The latter value is less of Fermi energy obtained earlier for PANI-SA, PANI-CSA and PANI-AMPSA.

Intrinsic conductivity and mechanism of charge transfer in PANI with doping level lying above the percolation threshold depend on the structure and number of counterion introduced into a polymer. At high doping level the saturation of spin-packets decreases significantly due to the increase in direct and cross spin-spin and spin-lattice interactions. Besides, Dysonian term appears in EPR spectra of such polymers due to the formation of skin-layer on their surface. In contrast with the saturated dispersion EPR signal, the Dysonian line “feels” both types of charge carriers, spin polarons, and spineless bipolarons, as effective charge ensemble, diffusing through a skin layer. The number and dynamics of each type of charge carriers can differ; thus the electronic dynamics properties of the sample should depend on its doping level. In order to determine this correctly the analysis of both the *dc* and *ac* conductivities is required.

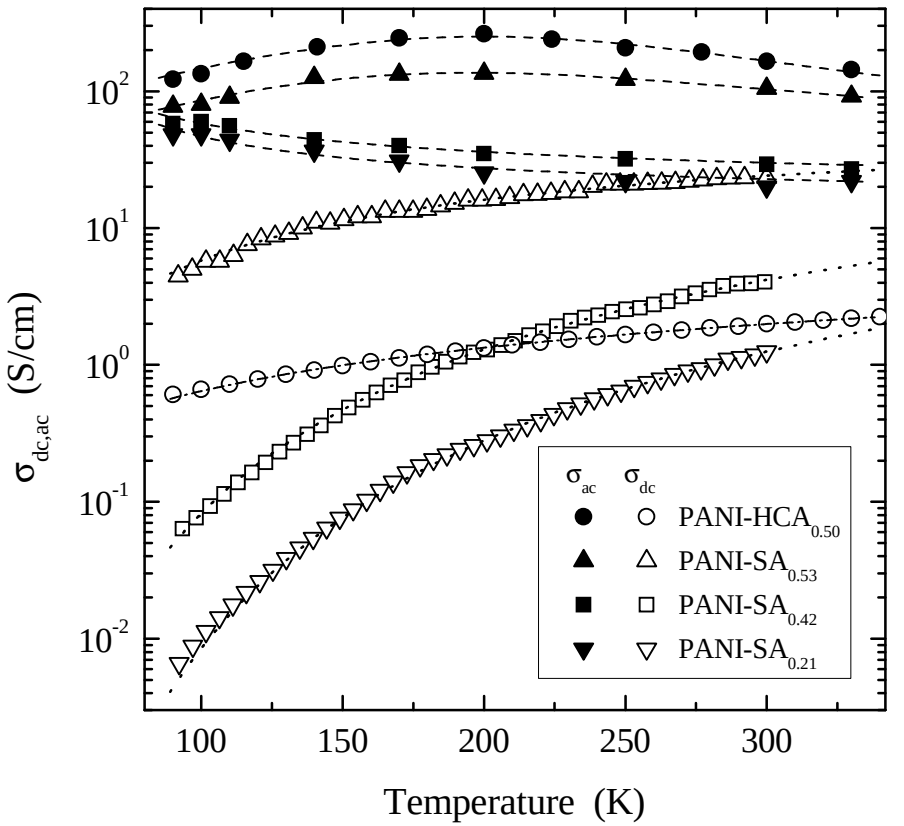

Figure 14. Temperature dependency of *ac* (filled symbols) and *dc* (open symbols) conductivity calculated from Dyson-like EPR line of the PANI-HCA and PANI-SA samples with different doping levels. Top-down dotted lines present the dependences calculated from Eq.(26) with respective with $k_1 = 9.2 \cdot 10^3$ S K$^{0.5}$/cm, $T_0 = 2.8 \cdot 10^3$ K, $k_2 =$ 0.53 S/K cm, $E_{ph} = 0.042$ eV, $k_1 = 3.5 \cdot 10^4$ S K$^{0.5}$/cm, $T_0 = 1.1 \cdot 10^4$ K, $k_2 = 1.3 \cdot 10^{-2}$ S/K cm, $E_{ph} = 0.062$ eV, $k_1 = 7.3 \cdot 10^5$ S K$^{0.5}$/cm, $T_0 = 1.9 \cdot 10^4$ K, $k_2 = 9.2 \cdot 10^{-3}$ S/K cm, $E_{ph} = 0.063$ eV, and $d = 1$. Dash-dotted line shows the dependence calculated from the same equation with $k_1 = 8.4 \cdot 10^2$ S K$^{0.5}$/cm, $T_0 = 3.6 \cdot 10^3$ K, $k_2 = 0.51$ S/K cm, $E_{ph} = 0.048$ eV and $d = 1$. Top-down dashed lines show the dependences calculated from Eq.(28) with respective $\sigma_{0_1} = 1.47$ S cm^{-1} K^{-1}, $\sigma_{0_2} = 2.1 \cdot 10^{-2}$ S cm^{-1} K^{-1}, and $E_{ph}^{|} = 0.12$ eV, $\sigma_{0_1} = 0.86$ S cm^{-1} K^{-1}, $\sigma_{0_2} = 4.3 \cdot 10^{-2}$ S cm^{-1} K^{-1}, and $E_{ph}^{|} = 0.087$ eV, $\sigma_{0_1} = 0.48$ S cm^{-1} K^{-1}, $\sigma_{0_2} = 8.5 \cdot 10^{-3}$ S cm^{-1} K^{-1}, and $E_{ph}^{|} = 0.049$ eV and $\sigma_{0_1} = 0.41$ S cm^{-1} K^{-1}, $\sigma_{0_2} = 5.7 \cdot 10^{-3}$ S cm^{-1} K^{-1}, $E_{ph}^{|} = 0.052$ eV, and $\kappa = -1$.

The analysis shown that the *dc* conductivity in PANI-HCA and PANI-SA samples presented in Fig.14 *vs*. temperature can be described in the framework of the models of Q1D Variable Range Hopping (VRH) of charge carriers between crystalline high-conducting regions through amorphous bridges [111] and their scattering on the lattice optical phonons in metal-like clusters.

VRH mechanism of charge motion results in the following dependence of the *dc* and *ac* conductivity of a *d*-dimensional system on temperature [111,133]

$$s_{\mathrm{dc}}(T) = s_0 \exp\left[-\left(\frac{T_0}{T}\right)^{\frac{1}{\mathrm{d}+1}}\right], \tag{24}$$

$$\sigma_{\mathrm{ac}}(T) = \frac{1}{3}\pi e^2 k_{\mathrm{B}} T n^2(\varepsilon_{\mathrm{F}})\langle L\rangle^5 \omega_{\mathrm{e}}\left[\ln\frac{\omega_0}{\omega_{\mathrm{e}}}\right]^4 = \sigma_0 T, \tag{25}$$

where $\sigma_0 = 0.39\omega_0 e^2[n(\varepsilon_F)\langle L\rangle/(k_B T)]^{1/2}$ and $T_0 = 16/k_B n(\varepsilon_F) z\langle L\rangle$ at $d = 1$, $\sigma_0 = \omega_0 e^2[9/8\pi k_B T n^{3/2}(\varepsilon_F)/\langle L\rangle]^{1/2}$ and $T_0 = 18.1/k_B n(\varepsilon_F)\langle L\rangle^3$ at $d = 3$ in equation for *dc* conductivity, ω_0 is a hopping attempt frequency, z is the number of nearest-neighbor chains, $\langle L\rangle$ is the averaged length of charge wave localization function, and T_0 is the percolation constant or effective energy separation between localized states depending on disorder degree in amorphous regions. The conductivity is essentially determined by the phonon bath and by the distributional disorder of electron states in space and energy respectively above and below T_0. The distance R and average energy W of the charge carriers hopping are $R^{-4} = 8\pi k_B T n(\varepsilon_F)/9\langle L\rangle$ and $W^1 = 4\pi R^3 n(\varepsilon_F)/3$, respectively.

DC conductivity of the samples is a combination of Eqs.(14) and (24):

$$s_{\mathrm{dc}}^{-1}(T) = k_1^{-1} T^{\pm 0.5} \exp\left[\left(\frac{T_0}{T}\right)^{\frac{1}{\mathrm{d}+1}}\right] + k_2^{-1} T^{-1}\left[\sinh\left(\frac{E_{\mathrm{ph}}}{k_{\mathrm{B}} T}\right) - 1\right]^{-1}. \tag{26}$$

The parameters of Eq.(26) determined from the fitting of experimental data are summarized in Table 3. It is seen from the Table that both the percolation constant and lattice phonon energy of PANI-ES decrease at the increase of polymer doping level. A transition from localization to delocalization of charge carriers occurs when $\pi^2 t_\perp/32^{1/2} T_0$ is equal to a unit [28]. This value was calculated for PANI-

$SA_{0.21}$, PANI-$SA_{0.42}$, PANI-$SA_{0.53}$, and PANI-$HCA_{0.50}$ using $t_{\perp}$ = 0.29 eV [86] and T_0 determined to be 0.31, 0.53, 2.1, and 3.1 eV, respectively. An increase in this value with y means increasing the charge-carrier delocalization as a result of an increase in the interchain coherence. This value is higher than unity for heavily doped PANI-HCl [134], and decreases down to 0.1 – 0.4 for heavily doped derivatives of polyaniline, namely, poly(o-toluidine) and poly(o-ethylaniline) [135]. One can conclude that the insulator-to-metal transition in PANI-SA is of localization-to-delocalization type, driven by the increased structural order between the chains and through an increased interchain coherence. PANI-$SA_{0.53}$ and PANI-$HCA_{0.50}$, possess a more metallic behavior, and the properties of PANI-SA $y \le 0.42$ demonstrate it to be near an insulator/metal boundary. The inherent disorder present in slightly doped PANI keeps the electron states localized on individual chains. At low y the structural disorder in polyaniline localizes the charge to single chains (Curie-like carriers), and

Table 3. The k_1 (in S $K^{\pm 0.5}$/cm), T_0 (in K), k_2 (in S/K cm), $\hbar\omega_{ph}$ (in eV) values determined from the fitting of σ_{dc} by Eq.(26), and σ_{0_1} (in S/K cm), σ_{0_2} (in S/K cm), and $\hbar\omega_{ph}^{|}$ (in eV) ones determined from the fitting of σ_{ac} by Eq.(28) for different PANI samples.

Polymer	k_1	T_0	k_2	E_{ph}	σ_{0_1}	σ_{0_2}	$E_{ph}^{|}$
PANI-$SA_{0.21}$	$7.3\cdot10^5$	$1.9\cdot10^4$	$9.2\cdot10^{-3}$	0.063	0.41	$5.7\cdot10^{-3}$	0.052
PANI-$SA_{0.42}$	$3.5\cdot10^4$	$1.1\cdot10^4$	$1.3\cdot10^{-2}$	0.062	0.48	$8.5\cdot10^{-3}$	0.049
PANI-$SA_{0.53}$	$9.2\cdot10^3$	$2.8\cdot10^3$	0.53	0.042	0.86	$4.3\cdot10^{-2}$	0.087
PANI-$HCA_{0.50}$	$8.4\cdot10^2$	$3.6\cdot10^3$	0.51	0.048	1.5	$2.1\cdot10^{-2}$	0.12
PANI-$AMPSA_{0.4}$	$1.2\cdot10^3$	209	0.31	0.022	1.68	1.57	0.037
PANI-$AMPSA_{0.6}$	$1.1\cdot10^3$	277	0.18	0.020	1.62	0.76	0.039
PANI-$CSA_{0.5}$	$5.6\cdot10^3$	521	1.7	0.028	1.99	0.68	0.039
PANI-$CSA_{0.6}$	$5.5\cdot10^3$	753	0.29	0.024	2.27	0.64	0.036
PANI-pTSA$_{0.5}$ [a]					13.3	0.25	0.027
PANI-pTSA$_{0.5}$ [b]	26	$4.6\cdot10^4$	0.19	0.027	24.9	10.8	0.022

Notes: [a] determined at 3-cm waveband EPR, [b] determined at 2-mm waveband EPR.

the higher doping leads to the appearance of delocalized electron states (Pauli-like carriers). This holds typically for the formation in PANI-ES with $y \ge 0.21$ metal-like domains, according to the island model proposed by Wang and co-workers [27,30]. This is consistent with that drawn earlier on the basis of data obtained with TEM and X-ray-diffraction methods [77].

Activation energy of dipole-dipole interaction of a polaron with neighboring spins determined from Eq.(26) is near to that of superslow anisotropic librations obtained by the Saturation Transfer EPR (ST-EPR) method [48,49,136]. This means that macromolecular dynamics plays an important role in interacting processes taking place in spin reservoir. The lattice librations modulate the interacting spin exchange and consequently the charge transfer integral. Assuming that polaron is covered by both electron and excited phonon clouds, we can propose that both spin relaxation and charge transfer should be accompanied with the phonon dispersion. Such cooperating charge-phonon processes seem to be more important for the doped polymers the high-coupled chains of which constitute 3D metal-like clusters.

Aasmundtveit *et al.* [67] have shown that 3-cm waveband EPR line width and consequently the spin-spin relaxation rate of PC in PANI depend directly on its *dc* conductivity. The comparison of $\Delta B_{pp}(T)$ and $\sigma_{ac}(T)$ functions presented in Fig.6 and Fig.14 demonstrate the additivity of these values at least for the higher doped polymers. Besides, Khazanovich [137] have found that spin-spin relaxation depends on the number of spins on each polymer chain N_s and on the number of neighboring chains N_c with which these spins interact as follows:

$$T_2^{-1} = \frac{4\langle \Delta\omega^2 \rangle}{5\omega_0 N_s}\left[21\ln\frac{\omega_0}{\omega_e} + 18\ln N_c \right]. \qquad (27)$$

Using $T_2 = 1.7\cdot10^{-7}$ sec, $\Sigma_{ij} = 1.2\cdot10^{45}$ cm^{-6}, and $\omega_0 = 6.1\cdot10^{13}$ rad/s determined from experiment, a simple relation $N_c \approx 55\exp(N_s)$ of these values is obtained from Eq.(27). This means that at least seven interacting spins exist on each chain as spin-packet and interact with $N_c = 20$ chains, *i e.* spin and charge 3D hopping does not exceeds distance more than $3c_{3D}$.

Figure 14 exhibits the temperature dependence of the *ac* conductivity of highly doped PANI-SA and PANI-HCA samples determined from their Dysonian 2-mm EPR spectra using Eq.(19), Eq.(22), and Eq.(23) as well. The shape of the temperature dependences presented demonstrates non-monotonous temperature dependence with a characteristic point $T_c \approx 200$ K. Such a temperature dependency can be attributed to the above-mentioned interacting charge carriers with lattice phonons at high temperatures (the metallic regime) and by their Mott VRH at low temperatures (the semiconducting regime). In this case the charge transfer should consist of two successive processes, so then the *ac* conductivity should be expressed as a combination of Eq.(14) and Eq.(25)

$$s_{ac}^{k}(T) = \left(s_{0_1} T\right)^k + \left\{ s_{0_2} T \left[\sinh\left(\frac{E_{ph}^{|}}{k_B T} \right) - 1 \right] \right\}^k . \qquad (28)$$

Figure 14 shows that the experimental σ_{ac} values obtained for PANI-SA and PANI-HCA are fitted well by Eq.(28) with the appropriate parameters listed in Table 3. The energy determined for phonons in PANI sample lies near to that (0.066 eV) evaluated from the data obtained by Wang et al. [27,30].

RT σ_{ac} of heavily doped PANI-SA and PANI-HCA, estimated from the contribution of spin charge carriers, does not exceed 140 S/cm. This value is much smaller than $\sigma_{ac}(\omega_e \to \infty) \cong 10^7$ S/cm calculated theoretically [138]; however, it lies near that obtained for metal-like domains in PANI at 6.5 GHz [44]. The σ_{ac}/σ_{dc} ratio for these domains can be evaluated to be 80 for PANI-$HSA_{0.50}$ and 18, 7, and 4 for PANI-SA with y = 0.21, 0.42, and 0.53, respectively. Taking into account that the $\sigma_{ac} = \sigma_{dc}$ condition should be fulfilled for classic metals [110], one can conclude a better structural ordering of these domains in PANI-SA. Charge carriers diffuse along these polymer chains with the constant D_{1D} can be determined from relation $s_{ac} = e^2 n(\varepsilon_F) D_{1D} c_{1D}^2$ to vary within $5 \cdot 10^{13} - 1.1 \cdot 10^{14}$ rad/s at room temperature that exceeds at least by an order of magnitude D_{1D} determined above for slightly doped samples. The RT mean free path [110] $l_i = \sigma_{ac} m_c v_F/(Ne^2)$ calculated for the highly doped PANI-SA and PANI-HCA is near to 0.5 and 6.0 nm, respectively. These values are smaller than that estimated for oriented *trans*-PA [45], but also holds for extended electron states in these polymers as well. The energy of lattice phonons obtained from *ac* data lies near the energy J_{af} of the interaction between spins (see Table 2), that shows the modulation of spin-spin interaction by macromolecular dynamics in the system.

DC and *ac* conductivity of the highly doped PANI-CSA and PANI-AMPSA determined respectively by the *dc* conductometry method [85] and from the Dysonian spectra of the R_2 PC are given in Fig.15 as function of temperature. Charge carrier hops through amorphous part of the sample and then diffuses through its crystalline domain, so then the *dc* term of the total conductivity of the samples should be determined by 1D VDH between metal-like domains accompanied by the charge carriers scattering on the lattice phonons in these domains described by Eq.(14) and Eq.(24). These processes occur parallel, so the effective conductivity can be expressed by Eq.(26).

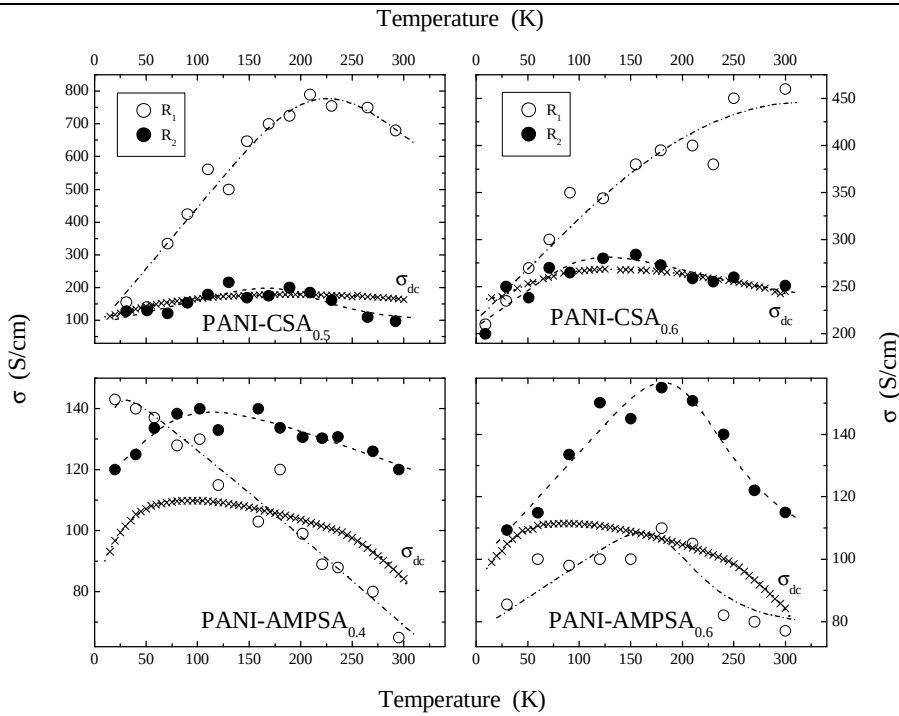

Figure 15. Temperature dependence of *dc* (open symbols) conductivity measured conductometrically and *ac* (filled symbols) conductivity determined from 3-cm, 8-mm, and 2-mm wavebands EPR Dysonian spectra of the R_2 paramagnetic centers stabilized in the PANI-AMPSA$_y$ and PANI-CSA$_y$ samples. Top-down dashed lines present the dependences calculated from Eq.(28) with κ = -1 and respective σ_{0_1} = 2.27 S/K cm, σ_{0_2} = 0.64 S/K cm, $E_{ph}^{|}$ = 0.036 eV, σ_{0_1} = 1.99 S/K cm, σ_{0_2} = 0.68 S/K cm, $E_{ph}^{|}$ = 0.039 eV, σ_{0_1} = 1.68 S/K cm, σ_{0_2} = 1.57 S/K cm, $E_{ph}^{|}$ = 0.037 eV, σ_{0_1} = 1.62 S/K cm, σ_{0_2} = 0.76 S/K cm, $E_{ph}^{|}$ = 0.039 eV as well as from Eq.(26) with d = 1 and respective k_1 = 5.5·10^3 S K$^{0.5}$/cm, T_0 = 753 K, k_2 = 0.29 S/K cm, E_{ph} = 0.024 eV, k_1 = 5.6·10^3 S K$^{0.5}$/cm, T_0 = 521 K, k_2 = 1.7 S/K cm, E_{ph} = 0.028 eV, k_1 = 1.1·10^3 S K$^{0.5}$/cm, T_0 = 277 K, k_2 = 0.18 S/K cm, E_{ph} = 0.020 eV, k_1 = 1.2·10^3 S K$^{0.5}$/cm, T_0 = 209 K, k_2 = 0.31 S/K cm, E_{ph} = 0.022 eV.

Figure 15 shows that *dc* conductivity of the polymers experimentally obtained is fitted well by Eq.(26) whose fitting parameters are summarized in Table 3. The v_F value was calculated for the PANI-CSA and PANI-AMPSA systems, to be 2.4·10^7 and 6.0·10^7 cm/s, respectively [85]. In contrast with other conducting polymers, lower T_0 parameter is characteristic for these samples. This

is evidence of the longer averaged length of charge wave localization function in the samples. Indeed, $<L>$ value was determined for PANI-$CSA_{0.6}$, PANI-$CSA_{0.5}$, PANI-$AMPSA_{0.6}$, and PANI-$AMPSA_{0.4}$, to be 17, 37, 264, and 239 nm, respectively. The $n(\varepsilon_F)$ increases in series PANI-$AMPSA_{0.4}$ → PANI-$CSA_{0.5}$ → PANI-$CSA_{0.6}$ → PANI-$AMPSA_{0.6}$.

AC conductivity of the polymers is also reflects the above mentioned successive mechanisms, so the experimental data can be circumscribed by Eq,(28). Indeed, it is seen from Fig.15 that the $\sigma_{ac}(T)$ dependences obtained experimentally for mobile R_2 PC are fitted well by Eq.(28) with the parameters summarized in Table 3. The energy determined for phonons in these PANI samples lies near to that obtained for other polymers [48,49] and evaluated (0.066 eV) from the data determined by Wang et al. for HCl-doped PANI [27,30]. It is evident that $E_{ph}^{|}$ and E_a obtained above for the PANI-$CSA_{0.5}$ sample lie near. This means that protons situated in crystalline domains indeed sense electron spin dynamics. The data obtained can be evidence of the contribution of the R_1 and R_2 PC in the charge transfer through respectively amorphous and crystalline parts of the polymers. RT σ_{ac} values determined from Dysonian spectra of R_2 PC lies near respective σ_{dc} values that is characteristic for classic metals. The $<L>$ and E_{ph} values determined above for mediatory doped samples correlate. This means that the higher the $<L>$ value, the stronger interaction of PC with phonons in metal-like crystallites. There is some tendency in the increase of RT σ_{dc} and σ_{ac} conductivities in the series PANI-$AMPSA_{0.6}$ → PANI-$AMPSA_{0.4}$ → PANI-$CSA_{0.5}$ → PANI-$CSA_{0.6}$ "feeling" by the R_2 PC. The data obtained can be evidence of indirect contribution of the R_1 PC and direct contribution of the R_2 PC in the charge transfer through respectively amorphous and crystalline parts of the polymers. RT σ_{ac} values determined from Dysonian spectra of R_2 PC lies near respective σ_{dc} values that is characteristic for classic metals.

Thus, main PC are localized in the highly doped PANI-CSA and PANI-AMPSA samples at low temperatures. This originates the Curie type of susceptibility of the samples and the VRH charge transfer between their polymer chains. The spin-spin exchange is stimulated at high temperature region due likely to the activation librations of the polymer chains [139,140]. Both pinned and delocalized PC are formed simultaneously in the regions with different crystallinity. An anti-ferromagnetic interaction in crystalline domains is stronger then that in amorphous regions of PANI-CSA and PANI-AMPSA. Charge transport between crystalline metal-like domains occurs through the disordered amorphous regions where the charge/spin carriers are more localized. The assumption that higher purity PANI coupled with homogeneous doping would

give rise to no EPR signal, characteristic of a purely bipolaronic matrix, is in contradiction with the increase of *ac* conductivity with spin concentration in polymer systems. Both PANI-CSA and PANI-AMPSA reveal better electronic properties over PANI-SA and PANI-HCA, as shown by their electrical conductivity which is both greater in magnitude and follows metallic temperature dependence. The change of conductivity with temperature is consistent with a disordered metal close to the critical regime of the metal-insulator transition with the Fermi energy close to the mobility edge [53,54].

Figure 16 shows the temperature dependence of σ_{dc} determined by the *dc* conductometry method for the PANI-*p*TSA$_{0.50}$. An analysis of these dependences leads to the conclusion that these polymers exhibit respectively 1D and 3D VRH at low temperature region, typical of a granular metal. As in case of other PANI, the σ_{dc} value is determined by strong spin-spin interaction at high temperatures. Experimental data is shown from Fig.16 to be well described by Eq.(26) with the parameters presented in Table 3.

The averaged length of charge wave localization $<L>$ lies in PANI-*p*TSA$_{0.50}$ near 11 nm and exceeds the effective radius of a quasi-metallic domain equal to 4 nm [141]. It can be due to closely electronic properties of the metal-like domains embedded into the polymer matrix. It allows to evaluate charge transfer integral $t_\perp$ in such domains from relation connecting T_0 values at 1D and 3D VRH [134], $T_0^{(3D)} = 256 T_0^{(1D)} \ln(2 T_0^{(1D)}/\pi t_\perp)$, to be 0.10 eV. The most probable carrier hopping range $R = (T_0/T)^{1/2}<L>/4$ is 34 nm in PANI-*p*TSA$_{0.50}$ at room temperature. The hopping energy W of a charge carrier in these polymers determined respectively in terms of the 3D VRH, $W = k_B(T_0T^3)^{1/4}/2$, and 1D VRH, $W = k_B(T_0T)^{1/2}/2$, models is 0.045 eV that is of the order of k_BT. The data make it possible to calculate the velocity of charge carriers $v_F = 4.0 \cdot 10^6$ cm/s moving near the Fermi energy with an energy of $\varepsilon_F = 0.34$ eV. The latter value lies near to that determined for PANI-CSA (0.4 eV) [20] and PANI-SA (0.5 eV) [83,86]. This is in agreement with the supposition earlier made by Pelster et al. [141] that the charge transport in PANI-*p*TSA takes place *via* two contributions: metallic conduction through a crystalline core of 8 nm, and thermally activated tunneling (hopping) through an amorphous barrier of 1-2 nm diameter.

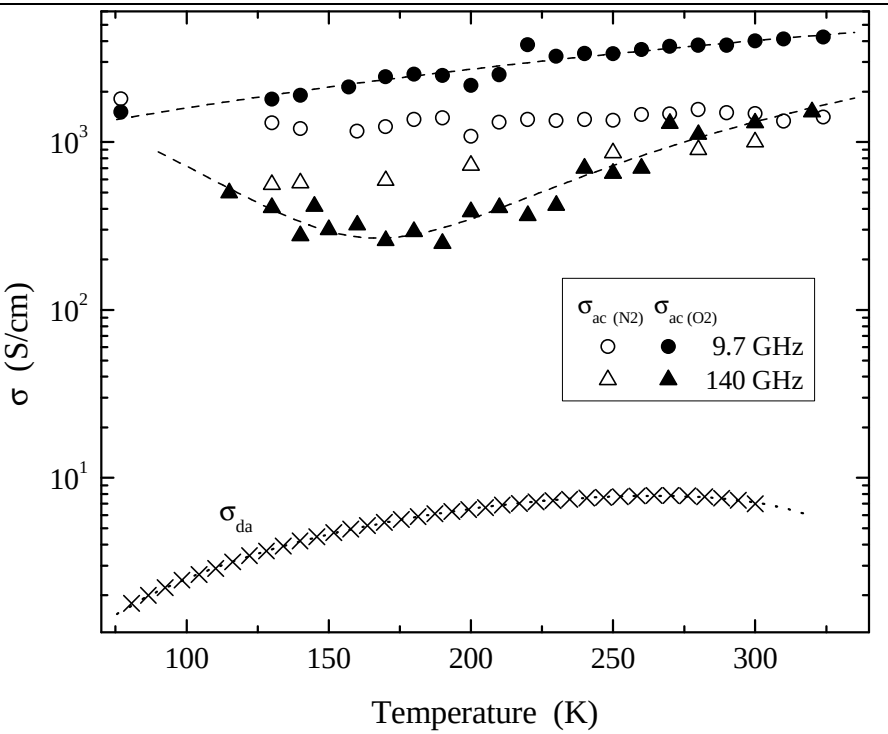

Figure 16. Temperature dependence of *dc* and *ac* conductivity determined from 3-cm and 2-mm waveband EPR Dysonian spectra of the PANI-*p*TSA$_{0.5}$ sample obtained in nitrogen (open symbols) and air (filled symbols) atmosphere. Dash-dotted line shows the dependence calculated from Eq.(26) with k_1 = 26 S K$^{-0.5}$/cm, $T_0 = 4.6 \cdot 10^4$ K, d = 3, k_2 = 0.19 S/K cm, $\hbar\omega_{ph}$ = 0.027 eV. Above and below dashed lines present the dependences calculated from Eq.(28) with σ_{0_1} = 13.3 S/K cm, σ_{0_2} = 0.25 S/K cm, $\hbar\omega_{ph}^{\downarrow}$ = 0.027 eV and σ_{0_1} = 24.9 S/K cm, σ_{0_2} = 10.8 S/K cm, $\hbar\omega_{ph}^{\downarrow}$ = 0.022 eV, respectively, and κ = 1.

Spin-lattice and spin-spin relaxation times measured by the saturation method [142] at 3-cm waveband EPR for the PANI-*p*TSA$_{0.50}$ are respectively $1.2 \cdot 10^{-7}$ and $3.1 \cdot 10^{-8}$ sec (in the nitrogen atmosphere) and $1.1 \cdot 10^{-7}$ and $1.6 \cdot 10^{-8}$ sec (in the air) [88,89]. If one supposes that the polarons in this polymer possess mobility and diffuse along and between polymer chains with the diffusion coefficients D_{1D} and D_{3D}, respectively, $D_{1D} = 3.5 \cdot 10^8$ and $D_{3D} = 1.1 \cdot 10^9$ rad/s (in the nitrogen atmosphere) and $D_{1D} = 8.1 \cdot 10^{11}$ and $D_{3D} = 2.3 \cdot 10^8$ rad/s (in the air) are evaluated from Eq.(8) and Eq.(9). A corresponding conductivities due to so possible polaron mobility calculated from Eq.(10) are respectively $\sigma_{1D} = 2.5 \cdot 10^{-4}$

S/cm, $\sigma_{3D} = 2.3 \cdot 10^{-4}$ S/cm and $\sigma_{1D} = 29$ S/cm, $\sigma_{3D} = 2.4 \cdot 10^{-3}$ S/cm. This means that $D_{1D} < D_{3D}$ in the sample without oxygen; however, the conductivity appears to be practically isotropic in character. The D_{1D}/D_{3D} ratio for the sample exposed to air increases to $\sim 10^4$, which substantially exceeds the value $D_{1D}/D_{3D} \sim 50$ obtained for highly doped PANI-HCA [56]. The conductivity of this sample also becomes anisotropic, $\sigma_{1D}/\sigma_{3D} \sim 10^4$, and is also determined mainly by the diffusion of paramagnetic center along the polymer chain. The data obtained can be compared with those evaluated from the Dysonian EPR spectra.

The σ_{ac} values determined for the PANI-*p*TSA$_{0.50}$ sample from its Dysonian 3-cm and 2-mm waveband EPR spectra by using Eq.(19), Eq.(22), and Eq.(23) are also shown in Fig.16 *vs*. temperature. An intrinsic conductivity of both the samples visibly increases at their exposition on air (Fig.16). RT conductivity obtained for *e.g*. the former sample at 3-cm waveband EPR is a two orders of magnitude higher than σ_{1D} and σ_{3D} calculated above in terms of Q1D polaron diffusion along the "single conducting chain" [56]. Hence, it may be concluded that the conductivity in these polymers, as in other polyanilines, is mainly determined by the mobility of 3D-delocalized electrons in metal-like domains in which paramagnetic polarons are localized on parallel chains because of their strong exchange interaction. The temperature dependence of intrinsic conductivity can be interpreted in terms of the VRH mechanism of charge carriers and their scattering on the polymer lattice phonons respectively in amorphous and crystalline phases of the samples. Analogous to other PANI, the charge carrier crosses these phases one after another, so the resulting conductivity should be described by Eq.(28). As Fig.16 shows, Eq.(28) approximates well the $\sigma_{ac}(T)$ conductivity evaluated for all the PANI samples exposed on air with the parameters listed in Table 3. The $E_{ph}^{|}$ value obtained for both the samples correlate with E_{ph} determined from the fitting of their $\sigma_{dc}(T)$ dependences in terms of the same charge transport mechanism (Table 3). This fact confirms additionally supposition above made on the existing of strong spin dipole-dipole interaction in crystalline domains.

A decrease in σ_{ac} with an increase in the registration frequency may as result of *e.g*. of the influence of external magnetic field on the spin-exchange process in the polymer or deeper penetration of MW field into the polymer bulk at 2-mm waveband EPR. Indeed, the intrinsic conductivity should be higher if the skin-layer is formed on metal-like domains with a smaller radius in PANI particles.

Therefore two types of PC are formed in PANI, as in case of main conducting polymers, polarons localized on chains in amorphous polymer regions and polarons moving along and between polymer chains. During the polymer

doping the number of the mobile polarons increases and the conducting chains become crystallization centers for the formation of the massive metal-like domains of strongly coupled chains with 3D delocalized charge carriers. This process is accompanied by the increase of the electron-phonon interaction, crystalline order, and interchain coupling. The latter factor plays an important role in the stabilizing of the metallic state, when both 1D electron localization and "Peierls instability" are avoided. Above the percolation threshold the interaction between spin charge carriers becomes stronger and their mobility increases, so part of the mobile polarons collapses into diamagnetic bipolarons. Besides, the doping changes the interaction of the charge carriers with the lattice phonons, and therefore the mechanism of charge transfer. It also results in an increase of the number and size of highly conducting domains containing charge carriers of different nature and mobility, which lead to an increase in the conductivity and Pauli susceptibility. This process is modulated by macromolecular dynamics, and is accompanied by an increase in the crystalline order (or dimensionality) and planarity of the system.

In the initial PANI the charges are transferred isoenergetically between solitary chains in the framework of the Kivelson formalism. The growth of the system dimensionality leads to the scattering of charge carriers on the lattice phonons. The charge 3D and 1D hops between these domains in the medium and heavily doped PANI, respectively. In heavily doped PANI the charge carriers are transferred according to the Mott VRH mechanism which is accompanied by their scattering on the lattice phonons. This is in agreement with the concept of the presence of 3D metal-like domains in PANI-ES rather than the supposition that 1D solitary conducting chains exist even in heavily doped PANI.

In contrast with PANI-SA and PANI-HCA characterized as a Fermi glass with electronic states localizes at the Fermi energy due to disorder, PANI-CSA, PANI-AMPSA, and PANI-*p*TSA are disordered metals on the metal-insulator boundary. The metallic quality of ES form of PANI grows in the series PANI-HCA → PANI-SA → PANI-*p*TSA → PANI-AMPSA → PANI-CSA.

The data presented show the variety of electronic processes, realized in PANI, which are stipulated by the structure, conformation, packing and the degree of ordering of polymer chains, and also by a number and the origin of dopants, introduced into the polymer. Among the general relationships, peculiar to these compounds are the following ones.

Spin and spineless non-linear excitations may exist as charge carriers in organic conducting polymers. The ratio of these carriers depends on various properties of the polymer and dopant introduced into it. The increase of doping level leads to the change of charge transfer mechanism. Conductivity in neutral or

weakly doped samples is defined mainly by interchain charge tunneling in the frames of the Kivelson formalisms, which is characterized by a high enough interaction of spins with several phonons of a lattice and leads to the correlation of Q1D spin motion and interchain charge transfer. These mechanisms ceases to dominate with the increase of doping level and the charge can be transferred by its thermal activation from widely separated localized states in the gap to close localized states in the tails of the valence and conducting bands. Therefore, complex quasi-particles, namely the molecular-lattice polarons are formed in some polymers because of libron-phonon interactions analogously to that it is realized in organic conjugated macromolecules. It should be noted that as conducting polymers have *a priori* a lower dimensionality as compared with molecular crystals, their dynamics of charge carriers is more anisotropic. In heavily doped samples the dominating is the interchain Mott charge transport, characterized by strong interaction of charge carriers with lattice phonons.

A higher spectral resolution at 2-mm waveband EPR provides a high accuracy of the measurement of magnetic resonance parameters and makes *g*-factor of organic free radicals an important informative characteristic. This allows the establishment of the correlation between the structure of organic radicals and their **g** tensor canonic values, providing the ability of PC identification in conducting polymers. The multifrequency EPR study allows obtaining qualitatively new information on spin carrier and molecular dynamics as well as on the magnetic and relaxation properties of polymer systems.

ACKNOWLEDGEMENTS

The author expresses his gratitude to Prof. Dr. G. Hinrichsen, Prof. A.P. Monkman and Dr. B. Wessling for the gift of polyaniline samples, to Dr. E.I. Yudanova and Dr. N.N. Denisov for the assistance in EPR experiments, as well as to Prof. Dr. H.-K. Roth for fruitful discussions. The **s**upport by the Russian Foundation of Basic Researches, grant 12-03-00148 is gratefully acknowledged.

References

[1] Bhadra, S, *Polyaniline: Preparation, Properties, Processing and Applications;* Lap Lambert Academic Publishing: 2010, 92 p.

[2] Wiederrecht, GP, Ed. *Handbook of Nanoscale Optics and Electronics;* 2010, 401 p.

[3] Syed, AA; Dinesan, MK; *Talanta* 1991, 38, 815.

[4] Bhadra, S; Chattopadhyay, S; Singha, NK; Khastgir, D; J. *Appl. Polym. Sci.* 2008, 108, 57-64.

[5] Jozefowicz, ME; Laversanne, R; Javadi, HHS; Epstein, AJ; Pouget, JP; Tang, X; MacDiarmid, AG; *Phys. Rev. B* 1989, 39, 12958-12961.

[6] Stafstrom, S; Bredas, JL; Epstein, AJ; Woo, HS; Tanner, DB; Huang, WS; MacDiarmid, AG; *Phys. Rev. Lett.* 1987, 59, 1464-1467.

[7] McCall, RP; Ginder, JM; Roe, MG; Asturias, GE; Scherr, EM; MacDiarmid, AG; Epstein, AJ; *Phys. Rev. B* 1989, 39, 10174-10178.

[8] Epstein, AJ; MacDiarmid, AG; Pouget, JP; *Phys. Rev. Lett.* 1990, 65, 664-664.

[9] Pouget, JP; Jozefowicz, ME; Epstein, AJ; Tang, X; MacDiarmid, AG; *Macromolecules* 1991, 24, 779-789.

[10] Trivedi, DC in *Handbook of Organic Conductive Molecules and Polymers;* H. S. Nalwa; Ed.;John Wiley: Chichester, 1997; Vol. 2, pp. 505-572.

[11] Ginder, JM; Richter, AF; MacDiarmid, AG; Epstein, AJ*; Solid State Commun.* 1987, 63, 97-101.

[12] Epstein, AJ; MacDiarmid, AG; *Journal of Molecular Electronics* 1988, 4, 161-165.

[13] Dai, LM; Lu, JP; Matthews, B; Mau, AWH; J. *Phys. Chem. B* 1998, 102, 4049-4053.

[14] Saprigin, AV; Brenneman, KR; Lee, WP; Long, SM; Kohlman, RS; Epstein, AJ; *Synth. Met.* 1999, 100, 55-59.

[15] Lee, K; Heeger, AJ; Cao, Y; *Synth. Met.* 1995, 72, 25-34.

[16] Yang, CY; Smith, P; Heeger, AJ; Cao, Y; Osterholm, JE; *Polymer* 1994, 35, 1142-1147.

[17] Wessling, B; Srinivasan, D; Rangarajan, G; Mietzner, T; Lennartz, W; *Eur. Phys. J. E* 2000, 2, 207-210.

[18] Reghu, M; Cao, Y; Moses, D; Heeger, AJ; *Phys. Rev. B* 1993, 47, 1758-1764.

[19] Yoon, CO; Reghu, M; Moses, D; Heeger, AJ; Cao, Y; *Phys. Rev. B* 1993, 48, 14080-14084.

[20] Lee, KH; Heeger, AJ; Cao, Y; *Phys. Rev. B* 1993, 48, 14884-14891.

[21] Lee, K; Heeger, AJ; Cao, Y; *Synth. Met.* 1995, 69, 261-262.
[22] Lee, K; Heeger, AJ; *Synth. Met.* 1997, 84, 715-718.
[23] Holland, ER; Pomfret, SJ; Adams, PN; Monkman, AP; *J. Phys.* 1996, 8, 2991-3002.
[24] Abell, L; Adams, PN; Monkman, AP; *Polymer* 1996, 37, 5927-5931.
[25] Abell, L; Pomfret, SJ; Adams, PN; Middleton, AC; Monkman, AP; *Synth. Met*. 1997, 84, 803-804.
[26] *Handbook of Organic Conductive Molecules and Polymers*; John Wiley & Sons: Chichester, New York, 1997, Vols.1-4.
[27] Wang, ZH; Li, C; Scherr, EM; MacDiarmid, AG; Epstein, AJ; *Phys. Rev. Lett*. 1991, 66, 1745-1748.
[28] Wang, ZH; Ray, A; MacDiarmid, AG; Epstein, AJ; *Phys. Rev. B* 1991, 43, 4373-4384.
[29] Monkman, AP; Adams, P; *Synth. Met.* 1991, 41, 627-633.
[30] Wang, ZH; Scherr, EM; MacDiarmid, AG; Epstein, AJ; *Phys. Rev. B* 1992, 45, 4190-4202.
[31] Reghu, M; Cao, Y; Moses, D; Heeger, AJ; *Synth. Met.* 1993, 57, 5020-5025.
[32] Adams, PN; Laughlin, PJ; Monkman, AP; Bernhoeft, N; *Solid State Commun*. 1994, 91, 875-878.
[33] Joo, J; Chung, YC; Song, HG; Baeck, JS; Lee, WP; Epstein, AJ; MacDiarmid, AG; Jeong, SK; *Synth. Met.* 1997, 84, 739-740.
[34] Wessling, B in *Handbook of Organic Conductive Molecules and Polymers;* H. S. Nalwa; Ed.;John Wiley & Sons: Chichester, 1997; Vol. 3, pp. 497-632.
[35] Adams, PN; Laughlin, PJ; Monkman, AP; *Synth. Met.* 1996, 76, 157-160.
[36] Epstein, AJ; Ginder, JM; Zuo, F; Bigelow, RW; Woo, HS; Tanner, DB; Richter, AF; Huang, WS; MacDiarmid, AG; *Synth. Met.* 1987, 18, 303-309.
[37] Fite, C; Cao, Y; Heeger, AJ; *Solid State Commun*. 1989, 70, 245-247.
[38] Zuo, F; Angelopoulos, M; MacDiarmid, AG; Epstein, AJ; *Phys. Rev. B* 1987, 36, 3475-3478.
[39] MacDiarmid, AG; Epstein, AJ; *Faraday Discuss*. 1989, 88, 317.
[40] Epstein, AJ; MacDiarmid, AG; *Synth. Met.* 1991, 41, 601-606.
[41] Cromack, KR; Jozefowicz, ME; Ginder, JM; Epstein, AJ; McCall, RP; Du, G; Leng, JM; Kim, K; Li, C; Wang, ZH; Druy, MA; Glatkowski, PJ; Scherr, EM; MacDiarmid, AG; *Macromolecules* 1991, 24, 4157-4161.
[42] Wang, ZH; Javadi, HHS; Ray, A; MacDiarmid, AG; Epstein, AJ; *Phys. Rev. B* 1990, 42, 5411-5413.
[43] Grosse, P, *Free Electrons in Solids (Russ);* Mir: Moscow, 1982, 270 p.

[44] [44] Joo, J; Oh, EJ; Min, G; MacDiarmid, AG; Epstein, AJ*; Synth. Met.* 1995, 69, 251-254.
[45] Kivelson, S; Heeger, AJ; *Synth. Met.* 1988, 22, 371-384.
[46] Krinichnyi, VI, *2-mm Wave Band EPR Spectroscopy of Condensed Systems*; CRC Press: Boca Raton, 1995, 223 p.
[47] Mizoguchi, K; Kuroda, S in *Handbook of Organic Conductive Molecules and Polymers*; H. S. Nalwa; Ed.;John Wiley & Sons: Chichester, New York, 1997; Vol. 3, pp. 251-317.
[48] Krinichnyi, VI; *Russ. Chem. Bull.* 2000, 49, 207-233.
[49] Krinichnyi, VI; *Synth. Met.* 2000, 108, 173-222.
[50] Menardo, C; Genoud, F; Nechtschein, M; Travers, JP; Hani, P in *Electronic Properties of Conjugated Polymers, Springer Series in Solid State Sciences;* H. Kuzmany; M. Mehring, and S. Roth; Ed.;Springer-Verlag: Berlin, 1987; Vol. 76, p. 244.
[51] Lapkowski, M; Genies, EM; *J. Electroanal. Chem.* 1990, 279, 157-168.
[52] MacDiarmid, AG; Epstein, AJ, in *Science and Application of Conducting Polymers Series,* W.R. Salaneck, D.C. Clark, and E.J. Samuelson, Eds.,; Adam Hilger: Bristol, 1991, p. 117
[53] Sariciftci, NS; Heeger, AJ; Cao, Y; *Phys. Rev. B* 1994, 49, 5988-5992.
[54] Sariciftci, NS; Kolbert, AC; Cao, Y; Heeger, AJ; Pines, A; *Synth. Met.* 1995, 69, 243-244.
[55] Nechtschein, M in *Handbook of Conducting Polymers*; T. A. Skotheim; R. L. Elsenbaumer, and J. R. Reynolds; Ed.;Marcel Dekker: New York, 1997, pp. 141-163.
[56] Mizoguchi, K; Nechtschein, M; Travers, JP; Menardo, C; *Phys. Rev. Lett.* 1989, 63, 66-69.
[57] Mizoguchi, K; Nechtschein, M; Travers, JP; *Synth. Met.* 1991, 41, 113-116.
[58] Mizoguchi, K; Nechtschein, M; Travers, JP; Menardo, C; *Synth. Met.* 1989, 29, E417-E424.
[59] Mizoguchi, K; Kume, K; *Solid State Commun*. 1994, 89, 971-975.
[60] Mizoguchi, K; Kume, K; *Synth. Met.* 1995, 69, 241-242.
[61] Nechtschein, M; Genoud, F; Menardo, C; Mizoguchi, K; Travers, JP; Villeret, B; *Synth. Met.* 1989, 29, E211-E218.
[62] Inoue, M; Inoue, MB; Castillo-Ortega, MM; Mizuno, M; Asaji, T; Nakamura, D; *Synth. Met.* 1989, 33, 355.
[63] Iida, M; Asaji, T; Inoue, M; Grijalva, H; Inoue, MB; Nakamura, D; *Bull. Chem. Soc. Jpn*. 1991, 64, 1509-1513.
[64] Ohsawa, T; Kimura, O; Onoda, M; Yoshino, K; *Synth. Met.* 1992, 47, 151-156.

[65] Bartle, A; Dunsch, L; Naarmann, H; Schmeisser, D; Gopel, W; Synth. Met. 1993, 61 167.
[66] Nechtschein, M; Genoud, F; *Solid State Commun*. 1994, 91, 471-473.
[67] Aasmundtveit, K; Genoud, F; Houze, E; Nechtschein, M; Synth. Met. 1995, 69, 193-196.
[68] Kahol, PK; Dyakonov, AJ; McCormick, BJ; *Synth. Met.* 1997, 89, 17-28.
[69] Kahol, PK; Dyakonov, AJ; McCormick, BJ; *Synth. Met.* 1997, 84, 691.
[70] Kang, YS; Lee, HJ; Namgoong, J; Jung, B; Lee, H; *Polymer* 1999, 40, 2209-2213.
[71] Mizoguchi, K; Kachi, N; Sakamoto, H; Yoshioka, K; Masubuchi, S; Kazama, S; *Solid State Commun*. 1998, 105, 81-84.
[72] Houze, E; Nechtschein, M; *Phys. Rev. B* 1996, 53, 14309-14318.
[73] Dyson, FJ; *Phys. Rev. B* 1955, 98, 349-359.
[74] Monkman, AP; Bloor, D; Stevens, GC; *Journal of Physics D* 1990, 23, 627-629.
[75] Iida, M; Asaji, T; Inoue, MB; Inoue, M; *Synth. Met.* 1993, 55, 607-612.
[76] Lubentsov, BZ; Timofeeva, ON; Saratovskikh, SL; Krinichnyi, VI; Pelekh, AE; Dmitrenko, VV; Khidekel, ML; *Synth. Met.* 1992, 47, 187-192.
[77] Lux, F; Hinrichsen, G; Krinichnyi, VI; Nazarova, IB; Chemerisov, SD; Pohl, MM*; Synth. Met.* 1993, 55, 347-352.
[78] Roth, HK; Krinichnyi, VI; Makromolek. *Chem.-Macromolec. Symp.* 1993, 72, 143-159.
[79] Krinichnyi, VI*; Russ. Chem. Rev*. 1996, 65, 521-536.
[80] Krinichnyi, VI; Chemerisov, SD; Lebedev, YS; *Phys. Rev. B* 1997, 55, 16233-16244.
[81] Krinichnyi, VI; Chemerisov, SD; Lebedev, YS; *Synth. Met.* 1997, 84, 819-820.
[82] Krinichnyi, VI; Chemerisov, SD; Lebedev, YS*; Polym. Sci. A* 1998, 40, 826-834.
[83] Krinichnyi, VI; Nazarova, IB; Goldenberg, LM; Roth, HK; *Polym. Sci. A* 1998, 40, 835-843.
[84] Krinichnyi, VI; Konkin, AL; Devasagayam, P; Monkman, AP; *Synth. Met.* 2001, 119, 281-282.
[85] Kon'kin, AL; Shtyrlin, VG; Garipov, RR; Aganov, AV; Zakharov, AV; Krinichnyi, VI; Adams, PN; Monkman, AP; *Phys. Rev. B* 2002, 66, 075203/1-075203/11.
[86] Krinichnyi, VI; Roth, HK; Hinrichsen, G; Lux, F; Lüders, K; *Phys. Rev. B* 2002, 65, 155205/1-155205/14.
[87] Krinichnyi, VI; Roth, HK; Hinrichsen, G; *Synth. Met.* 2003, 135, 431-432.

[88] Krinichnyi, VI; Tokarev, SV; *Polym. Sci. A* 2005, 47, 261-269.
[89] Krinichnyi, VI; Tokarev, SV; Roth, HK; Schrödner, M; Wessling, B; *Synth. Met.* 2005, 152, 165-168.
[90] Krinichnyi, VI; Konkin, AL; Monkman, A; *Synthetic Metalls* 2012, 162, 1147–1155.
[91] Krinichnyi, VI; Yudanova, EI; Wessling, B; *Synth. Met.* 2013, 179, 67–73.
[92] Lux, F, *PhD Thesys, Technical University of Berlin*, 1993.
[93] Timofeeva, ON; Lubentsov, BZ; Sudakova, YZ; Chernyshov, DN; Khidekel, ML; *Synth. Met.* 1991, 40, 111-116.
[94] Adams, PN; Laughlin, PJ; Monkman, AP; Kenwright, AM; *Polymer* 1996, 37, 3411-3417.
[95] Adams, PN; Monkman, AP, United Kingdom *Patent No. 2287030* (1997).
[96] Adams, PN; Devasagayam, P; Pomfret, SJ; Abell, L; Monkman, AP; *J. Phys.* 1998, 10, 8293-8303.
[97] Buchachenko, AL; Vasserman, AM, *Stable Radicals* (Russ); Khimija: Moscow, 1973, 408 p.
[98] Carrington, A; McLachlan, AD, *Introduction to Magnetic Resonance with Application to Chemistry and Chemical Physics*; Harrer & Row, Publishers: New York, Evanston, London, 1967, 295 p.
[99] Long, SM; Cromack, KR; Epstein, AJ; Sun, Y; MacDiarmid, AG; *Synth. Met.* 1994, 62, 287-289.
[100] Krinichnyi, VI; *Appl. Magn. Reson.* 1991, 2, 29-60.
[101] Krinichnyi, VI; *J. Biochem. Bioph. Methods* 1991, 23, 1-30.
[102] Poole ChP; Electron Spin Resonance. A Comprehensive Treatise on Experimental Techniques, *Int. Sci. Publ.*, London, 1967, 922 p.
[103] Bernier, P in *Handbook of Conducting Polymers*; T. E. Scotheim; Ed.;Marcel Deccer, Inc.: New York, 1986; Vol. 2, pp. 1099-1125.
[104] Pelekh, AE; Krinichnyi, VI; Brezgunov, AY; Tkachenko, LI; Kozub, GI; Vysokomolekul. *Soedin.*, Seriya A 1991, 33, 1731-1738.
[105] Krinichnyi, VI; Pelekh, AE; Brezgunov, AY; Tkachenko, LI; Kozub, GI; *Mater. Sci. Engin.* 1991, 17, 25-29.
[106] Kurzin, SP; Tarasov, BG; Fatkullin, NF; Aseeva, RM; Vysokomolekul. *Soedin.*, Seriya A 1982, 24, 117.
[107] Abragam, A, *The Principles of Nuclear Magnetism*; Clarendon Press: Oxford, 1961, 599 p.
[108] Butler, MA; Walker, LR; Soos, ZG; *J. Chem. Phys*. 1976, 64, 3592-3601.
[109] Lebedev, YS; Muromtsev, VI, *EPR and Relaxation of Stabilized Radicals* (Russ); Khimija: Moscow, 1972, 255 p.

[110] Blakemore, JS, *Solid State Physics*; Cambridge University Press: Cambridge, 1985, 506 p.
[111] Mott, NF; Davis, EA, *Electronic Processes in Non-Crystalline Materials;* Clarendon Press: Oxford, 1979, 590 p.
[112] Kivelson, S; *Phys. Rev. Lett.* 1981, 46, 1344-1348.
[113] Kivelson, S; *Bull. Amer. Phys. Soc* 1981, 26, 383-383.
[114] Kivelson, S; *Phys. Rev. B* 1982, 25, 3798-3821.
[115] Devreux, F; Genoud, F; Nechtschein, M; Villeret, B in *Electronic Properties of Conjugated Polymers*; H. Kuzmany; M. Mehring, and S. Roth; Ed. Springer Series in Solid State Sciences;Springer-Verlag: Berlin, 1987; Vol. 76, pp. 270-276.
[116] Zuppiroli, L; Paschen, S; Bussac, MN; *Synth. Met.* 1995, 69, 621-624.
[117] Cao, Y; Li, SZ; Xue, ZJ; Guo, D; *Synth. Met.* 1986, 16, 305-315.
[118] Pietronero, L; *Synth. Met.* 1983, 8, 225-231.
[119] Javadi, HHS; Cromack, KR; MacDiarmid, AG; Epstein, AJ; *Phys. Rev. B* 1989, 39, 3579-3584.
[120] Long, AR; Balkan, N; *Philos. Mag. B* 1980, 41 287-305.
[121] El Kadiri, M; Parneix, JP in *Electronic Properties of Polymers and Related Compounds*; H. Kuzmany; M. Mehring, and S. Roth; Ed. Springer Series in Solid State Sciences;Springer-Verlag: Berlin, 1985; Vol. 63, p. 183.
[122] Parneix, JP; El Kadiri, M in *Electronic Properties of Conjugated Polymers;* H. Kuzmany; M. Mehring, and S. Roth; Ed. Springer Series in Solid State Sciences;Springer-Verlag: Berlin, 1987; Vol. 76, pp. 23-26.
[123] Molin, YN; Salikhov, KM; Zamaraev, KI, *Spin Exchange: Principles and Applications in Chemistry and Biology*; Springer: Berlin, 1980, 242 p.
[124] Vonsovskii, SV, *Magnetism* (Russ); Nauka: Moscow, 1971, 1031 p.
[125] Salavagione, H; Morales, GM; Miras, MC; Barbero, C; *Acta Polym.* 1999, 50, 40-44.
[126] Kahol, PK; Pinto, NJ; McCormick, BJ; *Solid State Commun.* 1994, 91, 21-24.
[127] Kahol, PK; Clark, GC; Hehring, M in *Conjugated Conducting Polymers;* H. Kiess; Ed.;Springer-Verlag: Berlin, Heidelberg, New York, 1992; Vol. 102, pp. 217-304.
[128] Chapman, AC; Rhodes, P; Seymour, EFW; *Proc. Phys. Soc.* 1957, B 70, 345-360.
[129] Beau, B; Travers, JP; Banka, E; *Synth. Met.* 1999, 101, 772.
[130] Beau, B; Travers, JP; Genoud, F; Rannou, P; *Synth. Met.* 1999, 101, 778.
[131] Pratt, FL; Blundell, SJ; Hayes, W; Nagamine, K; Ishida, K; Monkman, AP; *Phys. Rev. Lett.* 1997, 79, 2855-2858.

[132] Raghunathan, A; Kahol, PK; Ho, JC; Chen, YY; Yao, YD; Lin, YS; Wessling, B; *Phys. Rev. B* 1998, 58, R15955-R15958.

[133] Austin, IG; Mott, NF; *Adv. Phys*. 1969, 18, 41-102.

[134] Kahol, PK; Pinto, NJ; Berndtsson, EJ; McCormick, BJ; *J. Phys.* 1994, 6, 5631-5638.

[135] Pinto, NJ; Kahol, PK; McCormick, BJ; Dalal, NS; Wan, H; *Phys. Rev. B* 1994, 49, 13983-13986.

[136] Krinichnyi, VI in *Advanced ESR Methods in Polymer Research;* S. Schlick; Ed.;Wiley: Hoboken, NJ, 2006, pp. 307-338.

[137] [Khazanovich, TN; Vysokomolekul. *Soedin*. 1963, 5, 112.

[138] Lim, HY; Jeong, SK; Suh, JS; Oh, EJ; Park, YW; Ryu, KS; Yo, CH; *Synth. Met*. 1995, 70, 1463-1464.

[139] Krinichnyi, VI; *J. Phys. Chem. B* 2008, 112, 9746-9752.

[140] Krinichnyi, VI; *J. Chem. Phys.* 2008, 129, 134510-134518.

[141] Pestler, R; Nimtz, G; Wessling, B; *Phys. Rev. B* 1994, 49, 12718-12723.

[142] Poole, CP, *Electron Spin Resonance, A Comprehensive Treatise on Experimental Techniques*; John Wiley & Sons: New York, 1983, 780 p.

Advances in Materials Science Research

Volume 17

Contributors

M. T. Chevalier
J. S. Gonzalez
V. A. Alvarez
Romina Ollier
Matias Lanfranconi
Vera Alvarez
Yongsheng Zhang
Yuan Fang
Hengzhong Fan
Junjie Song
Tianchang Hu
Litian Hu
Svetlana Motyleva
Jan Brindza
Radovan Ostrovsky
Maria Mertvicheva
V. I. Krinichnyi
Csilla Varga

ISBN 978-1-62948-734-2

Maryann C. Wythers
Editor

www.novapublishers.com